Review

Olive Mill Wastewater Remediation: From Conventional Approaches to Photocatalytic Processes by Easily Recoverable Materials

Melissa G. Galloni [1,2], Elena Ferrara [1], Ermelinda Falletta [1,2,*] and Claudia L. Bianchi [1,2]

[1] Department of Chemistry, Università degli Studi di Milano, Via Camillo Golgi 19, 20133 Milan, Italy
[2] Consorzio Interuniversitario Nazionale per la Scienza e Tecnologia dei Materiali (INSTM), Via Giusti 9, 50121 Florence, Italy
[*] Correspondence: ermelinda.falletta@unimi.it; Tel.: +39-02-503114410

Abstract: Olive oil production in Mediterranean countries represents a crucial market, especially for Spain, Italy, and Greece. However, although this sector plays a significant role in the European economy, it also leads to dramatic environmental consequences. Waste generated from olive oil production processes can be divided into solid waste and olive mill wastewaters (OMWW). These latter are characterized by high levels of organic compounds (i.e., polyphenols) that have been efficiently removed because of their hazardous environmental effects. Over the years, in this regard, several strategies have been primarily investigated, but all of them are characterized by advantages and weaknesses, which need to be overcome. Moreover, in recent years, each country has developed national legislation to regulate this type of waste, in line with the EU legislation. In this scenario, the present review provides an insight into the different methods used for treating olive mill wastewaters paying particular attention to the recent advances related to the development of more efficient photocatalytic approaches. In this regard, the most advanced photocatalysts should also be easily recoverable and considered valid alternatives to the currently used conventional systems. In this context, the optimization of innovative systems is today's object of hard work by the research community due to the profound potential they can offer in real applications. This review provides an overview of OMWW treatment methods, highlighting advantages and disadvantages and discussing the still unresolved critical issues.

1. Introduction

Olive oil production is a fundamental sector for several European (EU) States, especially Spain, Italy, and Greece. In particular, Spain has the largest area of olive cultivation (estimated at *ca.* 2.47 million ha), followed by Italy (*ca.* 1.16) and Greece (about 0.81 million ha) [1,2]. However, olive oil production is responsible for several environmental concerns (soil contamination, underground seepage, water-body pollution, and odor emissions) due to poor waste management practices [3]. In this scenario, concerning olive mill wastewaters (OMWW), special attention must be paid to their high phenolic content, which is responsible for their antibacterial effect, phytotoxic effect, and dark colour.

Recently, phenols, fatty acids, and volatile acids have been recognized as potentially hazardous for environmental health: the former have pronounced antimicrobial and phytotoxic properties, whereas the latter show toxicity due to their long alkyl chain.

All these components make OMWW toxic to anaerobic bacteria, thus inhibiting conventional secondary and anaerobic treatments in municipal water plants. Furthermore, the high BOD (biological oxygen demand) and COD (chemical oxygen demand) levels, which

cannot be reduced by anaerobic digestion, represent a further threat to receivers [2,4]. Moreover, land spreading and treatment in evaporation ponds could lead to problems related to groundwater pollution. The use of olive oil waste in agriculture may also affect the acidity, salinity, N immobilization, microbial response, leaching of nutrients, and concentration of lipids, organic acids, and phenolic compounds [5].

Alternative approaches based on physical treatments, such as dilution, evaporation, centrifugation, or sedimentation guarantee a high level of OMWW purification. However, they are expensive and energy-consuming, thus leading to an exponential increase in the processing cost. The olive oil industry, in its current status, composed of small and dispersed factories, cannot bear such high costs [6–13].

In recent years, advanced oxidation processes (AOPs), including photolysis, photooxidation, Fenton, and photo-Fenton reaction, have emerged as promising alternatives for simplicity and high organic removal efficiencies [14–20]. In particular, heterogeneous photocatalysis seems to be a successful technology in water decontamination due to its non-toxicity, low cost, and mineralization efficacy. However, due to the OMWW matrices' complexity, it is not easy to develop and successively optimize efficient photocatalytic systems that are so far characterized by common limitations (i.e., difficult recovery, poor stability, low reusability, fast deactivation).

Based on these premises, in the present work, for the first time, we illustrate the conventional methods commonly used to treat OMWW along with their related advantages and limitations. Then, a critical insight on alternative strategies for developing efficient photocatalytic systems based on recoverable catalysts is proposed. The latters can be used as alternatives to conventional photocatalysts. This topic is of fundamental importance for the research community as shown by the hard work currently been done for developing novel devices with high potential in real applications, acting as a bridge between environmental protection and circular economy.

2. An Insight into the EU Legislation

Olive oil is the desired product of the olives industry. Unfortunately, olive mill pomace and wastewater represent undesired by-products, requiring proper disposal treatments because of their complex composition (Figure 1).

The present work aims at discussing only the production and treatment of OMWW. OMWW composition is influenced by different factors, i.e., extraction methods, olives' type and origin, climate conditions, and cultivation/processing practices [21]. In general, it can be mainly summarized as follows (Figure 1): *ca.* 80–83 wt.% consists of water, *ca.* 15–18 wt.% relates to organic compounds (mainly polyphenols, phenols, and tannins), and the remaining 2 wt.% contains inorganic matter (i.e., potassium salts and phosphates). Specifically, phenols levels in OMWW range from 1 to 8 $g \cdot L^{-1}$, whereas micronutrients and mineral nutrients mainly consist of K_2O, and P_2O_5, which can be found in considerable amounts (2.4–10.8 or 0.3–1.5 $g \cdot L^{-1}$ intervals, respectively) [2]. Thus, it is critical to design efficient treatment methods, aligned to precise legislative constraints, whose general panorama is described below.

Concerning the processing of olive residues, the reform of standard agricultural policy related to olive oil does not provide specific provisions for their management [1]. It should be noted that a significant part of EU legislation acts according to Directives. These latter are legislative acts, setting objectives that all EU countries must reach and translate into their national legislation. This means that the member Countries have to adopt and impose complementary measures that should be compliant with the EU directives.

Following this scenario, an example is setting the emission limits and environmental quality standards. Of course, every Country can adopt laws and regulations that can be very different compared to others. Still, in the end, international norms are necessary for a common strategy to manage olive waste. In general, EU legislation governs each member state's framework of national legislation. Several EU laws regulate waste management, and the Waste Framework Directive, WFD (2008/98/EC), acts as core legislation, including

hazardous waste and oil rules [22]. In addition, Landfill Directive 99/31/EC regulates landfill disposal [23]. In this case, the waste producer, such as the olive mill operator, is responsible for managing wastes up to their recovery and disposal [24].
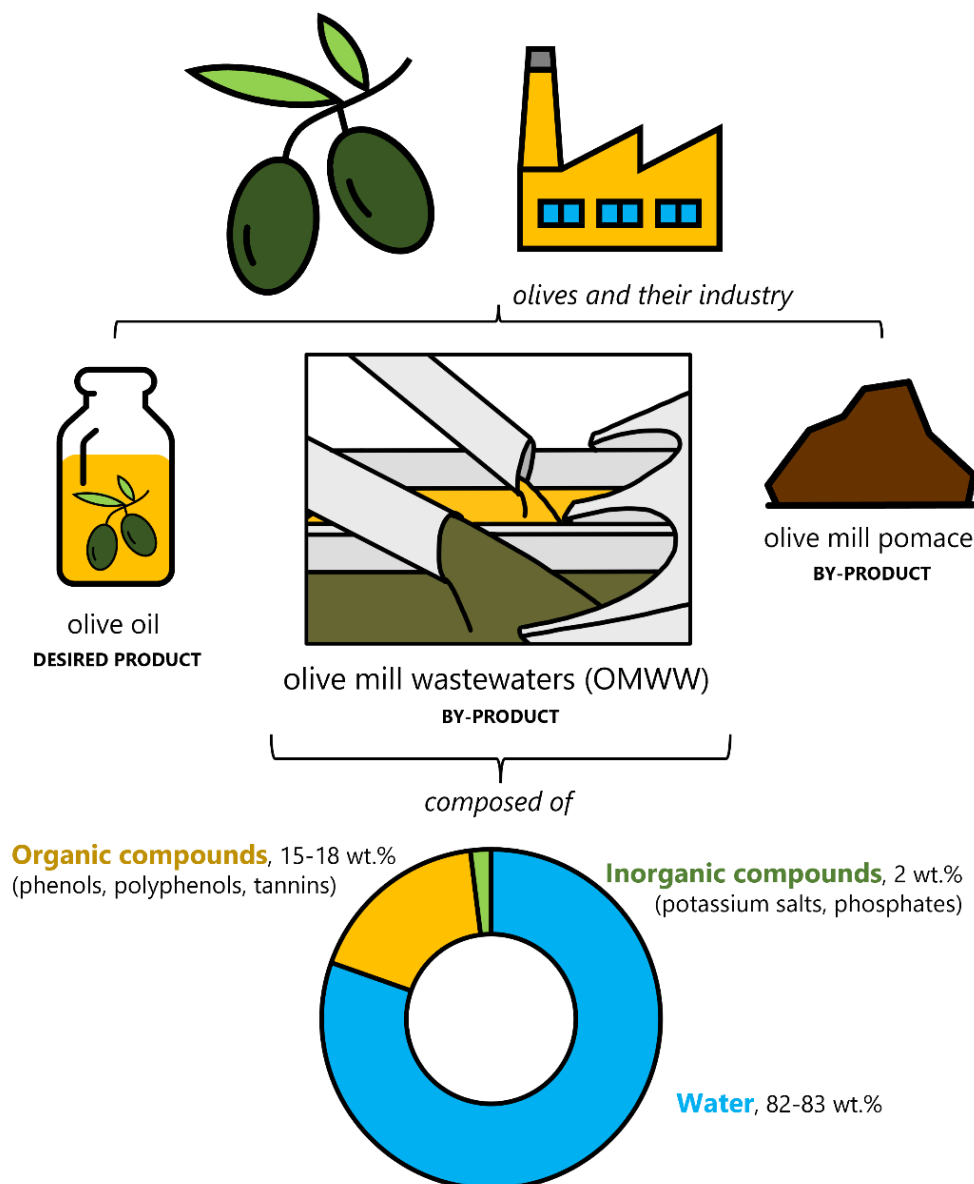

Figure 1. Scheme of products and by-products from the olive oil industry.

Here, the crucial point is to classify wastewaters as waste or by-products. If they are considered by-products, their further use as fertilizers with few restrictions is strongly recommended [25]. In this context, the EC Directive 2008/98 (point 22) clarifies the necessity to discriminate well between "waste" and "by-product", but unfortunately, considerable confusion is still present [22]. So, in many cases, law courts have to solve specific issues. To summarize, no EU legislation related to the management of OMWW exists today, and each EU country sets precise standard parameters.

3. Emerging Innovative Approaches for Olive Oil Production

Conventional techniques in olive oil extraction have not significantly changed in the last 25 years. Three main steps can be identified (Figure 2): crushing and malaxation, which mainly affect the oil quality and yield, and centrifugation [26,27].
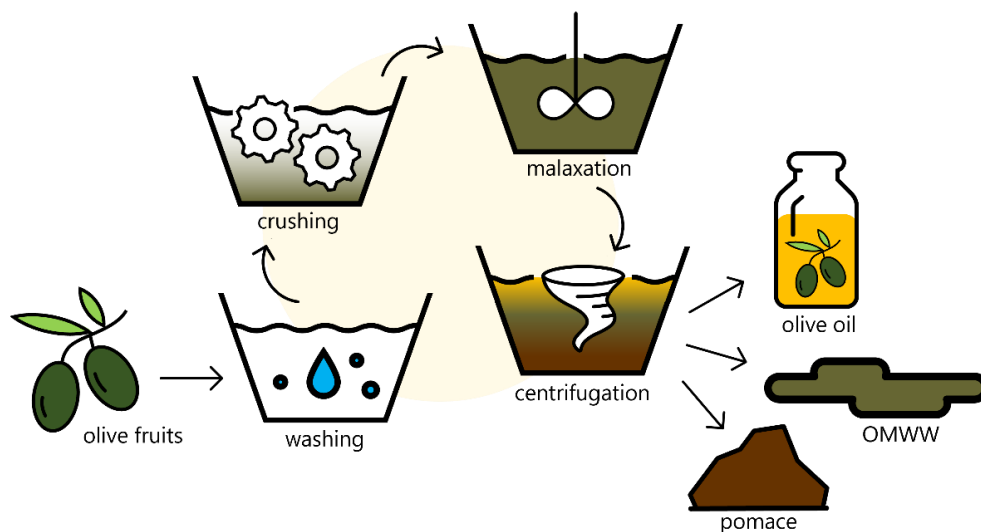
Figure 2. Scheme of olive oil production.

At first, stems, twigs, and leaves are separated from olive fruits [28]. These latter are then washed in a proper plant to remove dust, dirt, etc. In some plants, the washing water is recycled for the process after solid sedimentation or filtration, whereas in other cases, olives are directly processed without the washing step [29]. The next step involves malaxation: olives are ground up, mixed with/without their stones, and put in tanks, where the paste is divided into vegetation waters, pomace, and oil. Pomace, a brown-colored residue, is obtained by centrifugation and sedimentation after pressing olives [30,31]. Pomace mainly consists of skin pulp and pit fragments. Its separation is carried out using a horizontal decanter centrifuge and an olive oil press. The centrifuge step can be performed in two- or three-phases (Figure 3).
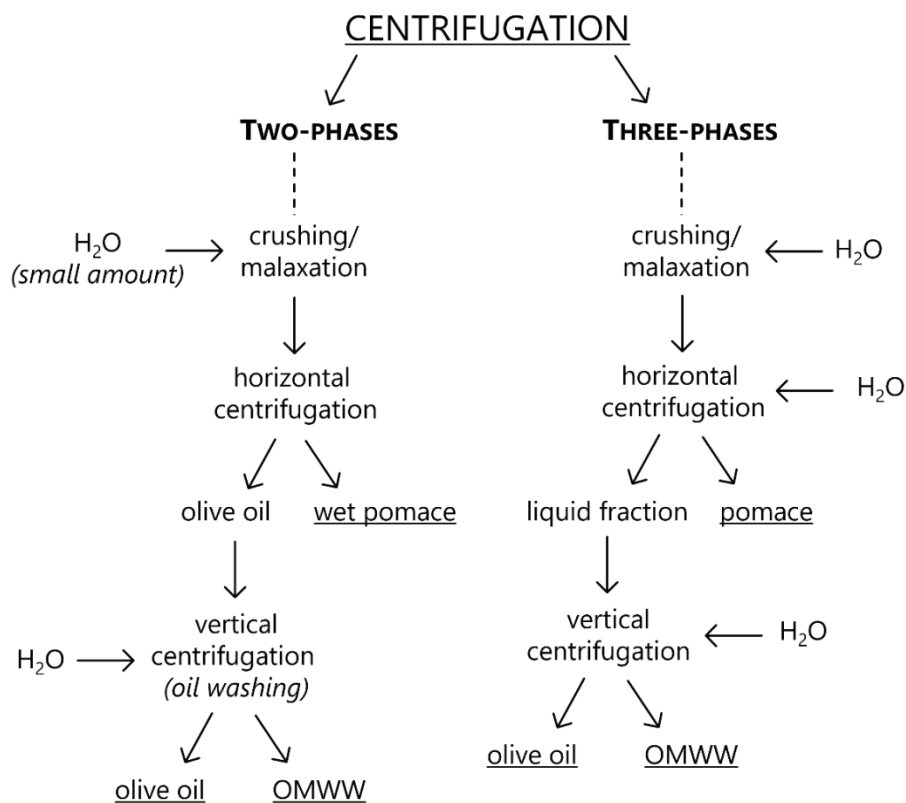

Figure 3. Scheme of two-phases and three-phases centrifugation strategies.

In the former case, wet pomace (also known as two-phase olive mill waste, TPOMW) and olive oil are obtained by horizontal centrifugation. Then, the obtained oil is centrifuged with water, producing olive oil and a small stream of OMWW [32,33]. In the latter, the olive paste is divided into pomace and a liquid fraction (olive oil *plus* OMWW), which is centrifuged with water to obtain high-quality olive oil and OMWW [32,33].

However, given the ever more urgent market demand, interesting novel methods characterized by minimal processing are currently the object of study. These approaches aim to obtain a final product with the same nutritional qualities in less time. In this context, numerous solutions, including the use of microwave, high-pressure processing, pulsed light, radio frequency, Ohmic heating, ultrasound, and pulsed electric field (PEF), have been investigated thanks to their advantages (enhanced extraction efficiency in reduced time with increased yield, and low energy consumption) [26,34–37].

Among them, ultrasound emerged as a powerful technology widely used in several extraction processes [37,38] and food processing methods (i.e., emulsification, filtration, crystallization, enzymes' and microorganisms' inactivation, thawing) [39,40]. Ultrasound can be applied to the olive paste to induce oil release from vacuoles in lower malaxation time. It has been demonstrated that high oil quality and yield are obtained [36,41–45].

Pulsed electric field (PEF) technology, used mainly in food science since 1960, consists of exposing food products (solid or liquid) to an electric field, inducing pore formation in cell membranes [46]. Recently, it has demonstrated its efficiency in reversible or irreversible permeabilization of cell membranes in different plants without causing significant temperature increase [34]. The possibility of maintaining low operating temperatures during the oil extraction process represents a valuable goal, as it allows the preservation of the product's organoleptic and nutritional characteristics.

An alternative to the two previous processes is microwave-assisted extraction (MAE), which represents a more efficient and successful strategy than the conventional ones because microwaves provide rapid heating and biological cell structure destruction. As a result, it leads to high-quality products with shallow energy requirements, inducing reduced environmental impact and financial costs [47].

Recently, emphasis has been placed on obtaining an increased Extra Virgin Olive Oil (EVOO) quality, preserving its sensory characteristic and favorable health properties. The quality of the EVOO strongly depends on the presence of phenolic and volatile compounds [43,44]. So, the development of emerging technologies to increase the oil yield while protecting and improving the bioactive oil compounds and quality is of fundamental importance.

Table 1 summarizes some interesting studies related to innovative technologies applied to olive oil extraction, including the maximum extraction yield obtained (i.e., the percentage value given by the ratio between the weights of the extracted oil and olives).

Table 1. Emerging extraction methods for olive oil production. Adapted from Ref. [48].

Olives' Variety	Used Technology [a]	Investigated Parameters	Dependent Variables	Maximum Extraction Yield (%) [b]	Ref.
Edremit	HPU	Ultrasound time, ultrasound temperature, malaxation time	Oil yield, acidity, peroxide value, and antioxidant properties	9	[26]
Coratina	HPU	Ultrasound application step (After crushing/ before crushing)	Olive paste temperature, energy balance, oil yield, quality indices of oil, minor compounds	16	[36]
Picual	HPU	Direct/indirect application of ultrasound	Olive paste temperature	16	[49]

Table 1. *Cont.*

Olives' Variety	Used Technology [a]	Investigated Parameters	Dependent Variables	Maximum Extraction Yield (%) [b]	Ref.
Picual	HPU	Continuous ultrasound application before centrifugation	Oil yield, quality indices, volatile and minor compounds, fatty acid composition	53	[50]
Edremit, Gemlik, Uslu	HPU	Ultrasound and malaxation time	Oil yield, UV absorbance values acidity, peroxide value, total phenolic content	68	[51]
Picual	HPU	Olive paste flow, HPU intensity, fruit temperature, olive moisture, and fat content	Olive paste temperature	17	[52]
Ogliarola Barese	HPU, MW	Thermal effect of US and MW	Malaxation time, oil yield, quality characteristics, and energy efficiency	17	[45]
Arbequina	PEF	PEF application	Oil yield, acidity, quality characteristics, total phenols, sensory properties	n.d. [c]	[35]
Chemlal	MW	Extraction time, acetic acid content in hexane, irradiation power	Oil yield, total phenols, quality parameters	6	[53]
Peranzana	MW	Malaxation time and MW	Energy consumption, oil yield, structure modifications of olive pastes	n.d. [c]	[54]
Coratina	HPU	Sonication time	Oil yield, oil quality indices, phenolic composition	n.d. [c]	[55]

[a] HPU: high-power ultrasound; PEF: pulsed electric field; MW: microwave; [b] expressed as percentage given by the ratio between the weights of the extracted oil and the olives; [c] not defined.

4. Olive Mill Wastewater Treatment

As reported above, OMWW is the waste of olive oil production characterized by high organic content and phytotoxic features mainly due to the presence of phenols, which are responsible for the olive oil's antimicrobial and antioxidant qualities. This makes waste biodegradation difficult in conventional treatment facilities (e.g., anaerobic digestion processes) that generally use microorganisms for waste biodegradation.

According to these premises, the OMWW treatment has faced several traditional approaches, which can be categorized as: disposal, physicochemical, biological, and advanced oxidation methods. Figure 4 schematizes their potentialities and weakness.
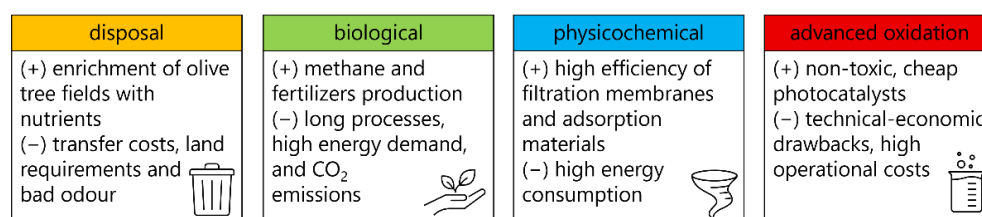

Figure 4. Main advantages/disadvantages of the standard technologies used for OMWW treatment.

As can be observed, all the mentioned technologies have specific advantages, but also cost problems. Therefore, some alternatives are currently the object of hard work by the research community. Among all the possibilities, one emerging and valid strategy is the OMWW steam reforming (OMWWSR), which permits valorization of wastes, producing green H_2, following the circular economy perspective [32]. It is a promising strategy in the view of the future projections of the H_2 market demand recently published by the International Energy Agency [56–58]. This method is described as having a high potential because of the environmental attractiveness of H_2, which is able to reduce CO_2 emissions in the atmosphere [56]. In this way, OMWWSR could contribute to air pollution reduction and, at the same time, valorize the waste from the olive oil industry [32]. However, this process still deserves to be properly studied and optimized because of some drawbacks affecting the catalyst formulation (e.g., low stability, deactivation, coke poisoning) [32].

The following paragraphs provide an accurate description of each traditional technology.

4.1. Disposal Methods

They mainly consist of treatment with calcium oxide (neutralization and coagulation) followed by the disposal of waterproof lagoons [59]. Unfortunately, they are affected by some disadvantages, such as foul odors, mosquitoes, and transfer costs because they require land far from residential areas. As an alternative, OMWW can be carried to fields of olive trees and then spread, thus enriching the soil with nutritive compounds [60].

4.2. Biological Methods

Bioremediation is a technology that exploits the metabolic potential of microorganisms to purify contaminated sites. It can be performed in a non-sterile and open area containing numerous organisms. Among these, bacteria have a central role in the process thanks to their ability to degrade pollutants. In addition, fungi and other components (e.g., grazing protozoa) can also affect the process [61]. All these species require nutrients (i.e., carbon, nitrogen, phosphates, metal traces) to survive, so they break down organic compounds to attain them. Bioremediation can occur under aerobic or anaerobic conditions [62]. In the former case, the survival of microorganisms is mainly due to the consumption of atmospheric oxygen. In contrast, in the latter, microorganisms gain food by breaking down chemical compounds in the soil [27].

In recent decades, OMWW has been used in this way, acting as substrate for microorganisms' growth by providing nutritive substances. Some yeast species (i.e., *Candida tropicalis, Yarrowia lipolytica*) together with bacteria of the *Azotobacter vinelandii, Pseudomonas, Sphingomonas, Ralstonia* species have been proven to be helpful in the OMWW aerobic biodegradation and detoxification [63–65]. By way of example, the activity of a free-living N_2-fixing bacterium, *Azotobacter vinelandii*, was investigated. In particular, OMWW was initially treated with calcium hydroxide to achieve the pH value of *ca.* 8–10 (stage I). Successively, it was mixed in a bioreactor in the presence of *Azotobacter vinelandii* (stage II). The process carried out according to the procedure reported by Arvanitoyannis et al. [27] resulted in an increasing level of nitrogen and its ammonium form throughout the whole remediation period. On the other hand, regarding phenols and sugar degradation, ca. 66–99% and 100% of phenols'abatement was observed after 3 and 7 days, respectively, whereas sugars were wholly degraded in only 3 days. Low phytotoxic features characterize the final product so it can be exploited as fertilizer [66].

In general, to reduce the high content of phenolic compounds in OMWW, water dilution represents a suitable strategy for a successful aerobic treatment. In fact, phenols are responsible for inhibition of microorganism growth [67,68]. Alternatively, OMWW could be mixed with additional waste and digested with the help of a solid substrate (i.e., straw, sesame bark, olive leaves, vineyard leaves, wood chips, animal manure) [69–71]. Then, when the phenol content of waste decreases, usually after 6–7 months, the final product can be exploited as fertilizer, giving profit [70,71]. Additionally, the composting stage could be coupled with physicochemical processes [72–74]. This last method requires high energy

demand and consequent high CO_2 emissions. However, the energy demand can be reduced thanks to simultaneous methane production [75].

4.3. Physicochemical Treatments

Among physicochemical treatments, dilution, evaporation, sedimentation, filtration, and centrifugation are commonly used to treat OMWW.

OMWW dilution is usually employed before biological treatments with the final aim to reduce its toxicity to microorganisms. On the other hand, evaporation and sedimentation result in a concentrated OMWW (*ca.* 70–75% more concentrated) thanks to both phase separation/dehydration and organic matter degradation [6,7]. In this context, solar distillation applied to OMWW can remove 80% COD in the distillate in 9 days, maintaining 25% water content [8].

Other strategies have also been investigated, mainly consisting of irreversible thermal treatments. This is the case with combustion and pyrolysis that require a reduced volume of waste and provide energy recovery. Still, unfortunately, they need expensive facilities, emit toxic substances into the atmosphere, and require an OMWW pre-concentration step [9,10].

Centrifugation and filtration increase the effluent pH and conductivity, removing the organic matter using phase separation and exclusion. Ordinarily, combining physical processes, coupled with coagulation/flocculation or adsorption techniques, gives rise to more efficient removal of organic matter. For example, it was found that when the sedimentation is followed by centrifugation and filtration, 21% and 15% decrease in COD and BOD, respectively, was observed, with the further 16% reduction in BOD due to the final filtration [11]. OMWW adsorption on activated clay causes an additional 71% COD reduction. However, a particular focus has to be put on the adsorption/desorption equilibrium since organic and phenolic features start to desorb after a precise contact time. The combination of treatment stages, i.e., settling, centrifugation, filtration, and adsorption on activated carbon, induce a maximum of 94% phenol abatement and 83% organic matter removal [12].

Regarding filtration, it is fundamental to point out that, besides the high efficiency of membranes, these processes require high operative pressures and energy consumption. However, proper membranes can be exploited to recover valuable by-products, such as phenols, which are mainly required for the pharmaceutical and chemical industry [13].

Lime treatment has been selected as a pre-treatment step for reducing OMWW polluting effect due to its inexpensiveness [76–79].

In this context, coagulation-flocculation is a very similar technology to lime treatment. Different coagulants (i.e., ferric chloride, polyelectrolytes) can be exploited [80]. On the other hand, electro-coagulation mainly consists of the suspension and precipitation of charged particles in the waste thanks to an applied voltage. Since this process is characterized by low cost and energy consumption, it is not so efficient in removing organic waste species.

4.4. Advanced Oxidation Methods

The addition of strong oxidizing agents can influence the efficiency of wastewater treatment, mainly in terms of the breakdown of recalcitrant and toxic compounds. In this context, high mineralization levels can occur depending on the oxidizing power of the agent employed and contact time. In recent decades, the scientific community has addressed the efforts to exploit advanced oxidation processes (AOPs) to treat industrial effluents and OMWW [14,15]. In general, AOPs combine ozone (O_3), light irradiation (UV, solar, visible), hydrogen peroxide (H_2O_2), and/or catalysts to produce unstable radical species able to degrade both organic and inorganic pollutants.

In electrolysis, the oxidation of the content of organic species directly occurs on the anode or indirectly by oxidizing agents present in the solution [81]. Over the years, several materials for anodes' production have been studied (i.e., Pt/Ir, Ti/IrO$_2$, Pt/Ti, and boron-doped diamond) [81–84]. However, this is a high-energy consuming approach. In contrast,

Fenton oxidation is based on the addition of Fenton's reagent (H_2O_2 and Fe(II)) into the waste [16]. In this case, the oxidation process is due to a cascade of different reactions in the solution. Although it is low energy consumption, H_2O_2 makes this technology quite expensive. The photo-Fenton method is very similar to the Fenton one, but the UV radiation accelerates Fe^{2+} regeneration, enhancing, as a consequence, the process efficiency. However, the necessity to employ UV radiation causes high energy consumption [85]. Supercritical water oxidation consists of waste oxidation in the presence or absence of catalyst above the water critical temperature and at high pressures [86–88]. It is a very efficient technology for organic content reduction, but the energy consumption is high due to the high temperatures and pressures required. Finally, ozonation employs O_3 as oxidant species for waste oxidation. It is not so efficient in the organic content reduction, but that of phenols is high. Unfortunately, using O_3 increases the process costs [89–91].

4.4.1. Photocatalytic Treatments

Photocatalysis can be described as an advanced oxidation process able to fully mineralize the contamination in liquid as well as the gas phase under room pressure and temperature [92]. Its efficiency is mainly due to the capability to generate powerful oxidizing agents [14,15,93,94]. In this way, the chemical transformation rate is enhanced by the chosen photocatalyst under light irradiation [95]. Following these perspectives, photocatalysis has found a successful application in the water decontamination field [96], providing promising results in the removal of a large variety of contaminants (e.g., aromatics, pesticides, drugs, oils) [97].

In this context, photocatalytic treatments can be applied in the field of OMWW degradation using both homogeneous and heterogeneous photocatalysts in the presence of UV, visible and solar light irradiation. In this class of treatments, photo-Fenton and solar-Fenton processes are also included [18,98,99].

In the following paragraphs, deeper insights into the current approaches used in the literature are reported with the aim of fully describing the scenarios related to these technologies.

UV Photocatalysis

Data summarized in Table 2 show how UV photocatalysis finds application in the OMWW treatment in the presence of both homogeneous and heterogeneous catalysts.

Table 2. State of the art of UV photocatalysis used to treat OMWW. Adapted from Reference [100].

OMWW Origin	Type of Process Treatment and Scale	Obtained Results	Ref.
Jordan	(i) O_3/UV or (ii) UV/O_3, followed by (iii) biodegradation—laboratory scale	COD removal efficiencies up to (i) 91% by UV/O_3 followed by biodegradation	[101]
Greece	Photocatalytic treatment with TiO_2 (Degussa P25)—laboratory scale	200 mg·L^{-1} COD residual and complete total phenol removal	[98]
Spain	pH-temperature flocculation + ferromagnetic core TiO_2 + UV photocatalysis—laboratory and pilot scale	58.3% COD and 27.5% total phenols removal efficiencies; overall COD removal efficiency up to 91%	[100,102]
Portugal	nano-TiO_2 immobilized in nonwoven paper—laboratory scale	90.8 $\pm$ 2.7% removal of the phenolic content	[103]
Italy	UV/TiO_2—laboratory and pilot scale	COD reduction around 50% upon 1.5 g·L^{-1} nanocatalyst dosage	[104,105]

Since 1972, titanium dioxide (TiO_2)-based photocatalysts have been investigated [106] and then widely used for their effective semiconductor features, enabling the removal of various pollutants in environmental remediation [107–109]. Interesting properties characterize these systems, like chemical stability, long-term stability, remarkable oxidation ability, and low-cost [110–112]. Heterojunction photocatalysts based on TiO_2 have been studied mainly for the mineralization of targeted pollutants into harmless products, thanks to the

generation of electron-hole (e^-/h^+) pairs if the semiconductor is under UV radiation [97]. In this frame, 2.80 V oxidizing power was produced by hydroxyl radicals produced during the photocatalytic step [96]. Besides the high chemical and physical stability of TiO_2, this material tends to go through phase transformation from anatase to rutile [113]. This induces a detrimental effect on the resulting TiO_2-materials because the rutile-phase has a lower surface area, negatively impacting the photocatalytic behaviour because of the (e^-/h^+) pairs' recombination [114].

In this regard, Chatzisymeon et al. explored the photocatalytic treatment of a three-phase OMWW remediation approach using TiO_2 in a laboratory-scale photoreactor. By properly optimizing the contact time, they observed the enhancement of COD removal. The product was a non-toxic effluent with 200 mg·L^{-1} COD organic content [98].

In this context, the high surface/volume ratio of TiO_2 nanoparticles, the possibility to dope them to increase the activation under solar irradiation, and the resistance to photo-corrosion are advantages related to the use of TiO_2-based photocatalysts.

This hitch can be minimized with the introduction of a second metal oxide component (e.g., MnO_2, NiO, La_2O_3, SiO_2, SnO_2, ZnO, ZrO_2), which has been recognized to induce significant degradation under UV irradiation [115–119], generating oxygen vacancies by the substitution of di- or tri-valent atoms by tetravalent atoms and providing particle-particle interaction [120]. In this context, very promising results have been obtained in terms of improved chemical stability and photocatalytic activities of the obtained materials, as demonstrated by many researchers in the last decades [121–123] and recently by Yaacob et al. for ZrO_2-TiO_2 materials [124].

However, TiO_2 has been recently recognized as a carcinogenic substance [125], so an unavoidable challenge is the development of alternative systems able to maintain the same or better photocatalytic activity. In this scenario, among all the potential candidates, one could be zinc oxide (ZnO), which is able to absorb a wide fraction of the solar spectrum and more than TiO_2 [126]. Many researchers have demonstrated its efficiency in the photodegradation of organic pollutants in water matrixes [127]. Additional features describe ZnO more than TiO_2 [128]; by way of example, it can be used in acidic or alkaline environments through proper treatment [129,130]. Moreover, the optimum pH for the ZnO process is *ca.* 7, whereas that of TiO_2 lies at acidic values, implying lower operational costs and higher efficiency than TiO_2 in the advanced oxidation of pulp mill bleaching wastewater [131], phenol and 2-phenyl phenol photooxidations [132,133]. In addition, it is highly photosensitive, stable, and possesses a bandgap of *ca.* 3.2 eV [134]. However, besides the numerous studies on using this material in this field, efforts to overcome drawbacks are necessary.

Visible/Solar Photocatalysis

As discussed so far, each step of the industrial sector for olive oil production implies high operational costs. In this context, any improvements introduced to reduce treatment costs must be carefully considered. Among these, for photocatalytic remediation, solar energy has to be properly developed, especially in the Mediterranean countries, with the final aim of cost-effectiveness.

Visible/solar photocatalytic strategies employ adequately designed heterogeneous and homogeneous photocatalysis, photo-Fenton, and solar-Fenton reagents. Some examples are reported in Table 3.

Gernjak et al. investigated OMWW from Portugal and Spain by solar photocatalysis [105]. In more detail, two solar reactors i were employed at pilot scale: (i) a conventional compound parabolic collector type (CPC); (ii) an open non-concentrating falling film reactor (FFR). Different solar photocatalytic systems were tested, but the photocatalyst with the higher amount of Fe (10 mM) showed the most increased activity.

Table 3. State of the art in visible/solar photocatalytic processes for OMWW treatment. Adapted with permission from Reference [135].

OMWW Origin	Type of Process Treatment and Scale	Obtained Results	Ref.
Spain and Portugal	(i) Solar photocatalysis with TiO_2 or added peroxydisulphate, or (ii) solar photo-Fenton—pilot plant	(i) Solar photocatalytic systems did not present sufficientefficacy (ii) 85% COD and up to 100% phenols concentration removal	[105]
Italy	(i) Centrifugation + solar photolysis, or (ii) centrifugation + solar modified photo Fenton—laboratory scale	(ii) COD and phenolics removal efficiencies up to 29.3% and 63.6%	[136]
Italy	Fenton preceded by coagulation—laboratory scale	85% COD removal (2 h)	[137]
Portugal	Biological (fungi *Pleurotus sajor caju*) and photo-Fenton oxidation—laboratory scale	COD removal efficiency up to 76% and total phenols up to 92%	[99]
Cyprus	Coagulation–flocculation, extraction of phenolics and post-oxidation by photo Fenton—laboratory scale	COD removal about $73 \pm 2.3\%$ and total phenols of $87 \pm 3.1\%$	[18]
Turkey	Sequential adsorption, biological and photo-Fenton treatment—laboratory scale	99% phenols reduction and 90% total organic content	[138]
Spain	UV/H_2O_2—laboratory scale	COD removal of 40–48% (30 min)	[139]

Ruzmanova et al. studied the photocatalytic treatment of a three-phase OMWW photodegradation process using reusable N-doped TiO_2 sol-gel compounds, demonstrating the higher activities of doped-catalysts compared to the non-doped ones, reaching a COD removal more elevated than 60% [140]. Additionally, N-doped materials maintain high efficiency when used for several cycles.

In addition, the role of photochemistry in the Fenton-like process is gaining attention thanks to ultraviolet and/or visible light to reduce the catalyst loading, enhancing the catalytic behaviour. In particular, Gernjak et al. investigated OMWW treatment processes by solar-photo Fenton approach on a pilot-plant scale, successfully removing up to 85% COD and 100% phenols [105].

Andreozzi et al. proposed an OMWW treatment based on a three-phase method exploiting (i) centrifugation followed by solar photolysis, (ii) centrifugation and solar photo-Fenton, and (iii) centrifugation coupled with solar photo-Fenton and ozonation. In this context, the ferric catalyst is responsible for COD and phenol removal (up to *ca.* 30% and 64%, respectively) [136].

Rizzo et al. investigated OMWW treatment by photo-Fenton, preceded by coagulation. In this case, the maximum efficiency of organic matter removal was *ca.* 95% in 1 h [137].

Justino et al. studied the combination of fungi *Pleurotus sajor caju* and photo-Fenton oxidation [99]. The treatment by fungi confirmed the reduction of OMWW toxicity towards *Daphnia longispina* and resulted in 72.9% total phenolic compounds removal and 77% COD reduction. When the treatment is preceded by photo-Fenton oxidation, the biological treatment with fungi is more efficient.

Papaphilippou et al. proposed a treatment process for OMWW by coupling coagulation–flocculation and Fenton oxidation. Following the photo-Fenton oxidation, COD and phenol removals were approximately 73% and 87%, respectively [18].

Finally, Aytar et al. reached 99% phenol and 90% total organic content reduction using adsorption, biological (*T. versicolor*), and photo-Fenton treatment in sequence [138].

Considering the depicted scenarios, it emerges that a proper comparison among the performances of the studied technologies to treat OMWW is not a trivial task. Indeed, the numerous variables in play (i.e., OMWW origin, process type and operative conditions, used scale) do not allow identification of a method that guarantees the best results in terms of OMWW removal. Only a rough evaluation in terms of COD removal can be done, but in this case, all the advantages and/or drawbacks of each strategy must be considered. In general, looking at the COD removal values reported in Table 3, interesting results were

obtained when working on a laboratory scale and in pilot plants, suggesting promising avenues that deserve to be investigated.

5. From Conventional to Easily Recoverable Magnetic Photocatalysts

As described in the previous sections, many approaches have been investigated for OMWW treatment [124,141–146]. Still, most of them suffer from not trivial and not negligible drawbacks (i.e., expensive maintenance, lateness in the separation time, high retention time).

In this regard, technologies based on photocatalysis can be advantageous for their environmental friendliness and high oxidation efficiency [147–149]. To develop even more efficient photocatalytic systems for real applications, research continuously moves the efforts toward exploring different materials.

Conventional nano-or micro-powder photocatalysts are developed for continuous, safe, and efficient photocatalytic reactions. Still, at the same time, their use is limited by the difficult separation and recovery from the reaction mixture for their sustainable reuse [150,151]. The recovery cost could invalidate the technology from an economic viewpoint [152]. To overcome this issue, the introduction of magnetic features in photocatalytic systems seems to be one of the best solutions, giving the possibility to maintain the catalytic performances of samples while making their separation from the reaction a more accessible medium.

Several approaches have been recently explored to develop advanced magnetic photocatalytic materials for wastewater remediation. However, unfortunately, few studies have mainly focused on applying these materials in the treatment of OMWW.

For this purpose, different magnetic nanoparticles (i.e., γ-Fe_2O_3, Fe_3O_4, MFe_2O_4, where M = Mg, Ni, Zn, Cu, Co) have been introduced in photocatalysts, giving rise to composite materials with magnetic features [153–156]. In this context, electron and hole migration between the magnetic and semiconductor components results in the separation of the photo-induced charge carriers, enhancing the light absorption ability [153–156]. This class of innovative materials has been studied regarding several pollutants in wastewater decontamination. Shen et al. prepared Fe_3O_4@TiO_2@Ag-Au microspheres with promising magnetic and photocatalytic properties [157]. Singh et al. immobilized $BiOI$/Fe_3O_4 photocatalyst on graphene oxide to degrade 2, 4-dinitrophenol [158]. Furthermore, the potentialities of other magnetic composite photocatalysts have been explored, such as $Cu_2V_2O_7$/$CoFe_2O_4$/g-C_3N_4 [159], $MnFe_2O_4$/SnO_2 [160], MoO_3/$CoFe_2O_4$ [161]. As already mentioned by Ma et al., the research efforts in this field have resulted in the development of several simple and magnetic photocatalytic materials, such as magnetic bismuth-based photocatalysts [162]. In addition, Ruzmanova et al. developed magnetic core TiO_2/SiO_2/Fe_3O_4 nanoparticles to degrade organic compounds in OMWW. 1.5 g·L^{-1} of catalyst dosage optimized the photodegradation process, providing high efficiency and an easy catalyst recovery [140]. Successively, Vaiano et al., using ferromagnetic N-TiO_2/SiO_2/Fe_3O_4 nanoparticles, achieved 64% phenol removal and 55% TOC reduction after an irradiation time of 270 min, as well as good stability of the photocatalytic materials after four operation/regeneration cycles [163]. Hesas et al. explored a magnetically separable Fe_3O_4 on modernite zeolite to purify OMWW from Kermanshah. They identified the key parameters influencing COD and BOD removal: pH (optimized at the value of 7.8) and turbidity of the treated solution. In addition, in this case, the regenerated Fe_3O_4/mordenite zeolite could be reused for five consecutive cycles [164].

In addition, the research community is currently working hard on novel alternatives.

6. Perspectives

Considering the high impact of OMWW treatment on the environment and human health, all the sustainability and circular economy principles should be adequately assessed. In this context, perspectives related to the development of efficient, sustainable alternatives to nano- or micro-sized photocatalysts to treat OMWW (Figure 5) can be mainly divided

into two categories: (i) eco-friendly materials (mainly characterized by magnetic features) already investigated in the treatment of several "model pollutants"; and (ii) other emerging eco-friendly materials (floating devices, membranes).
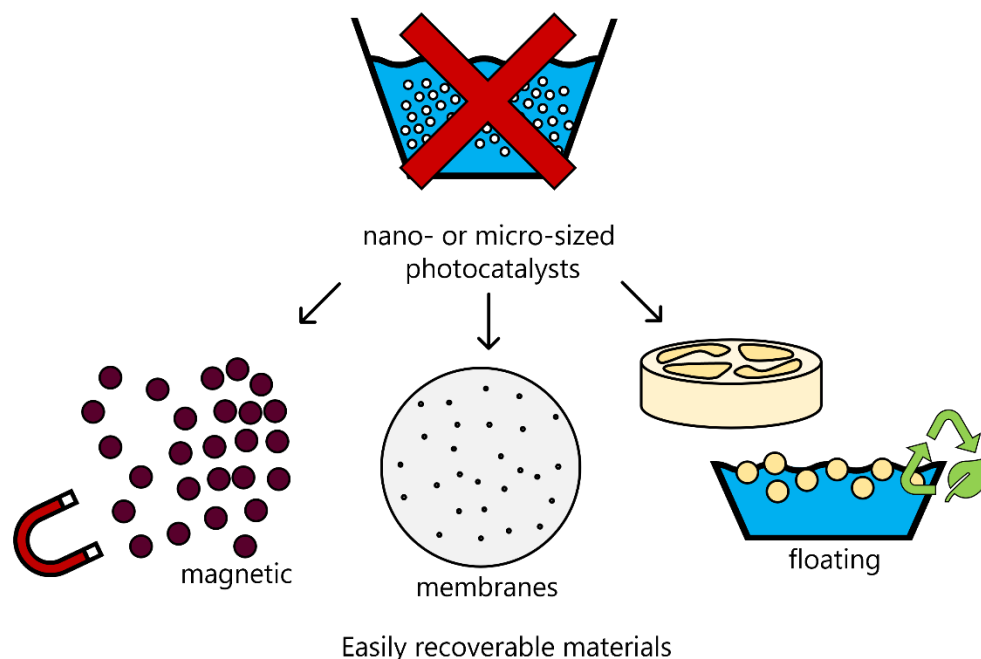

Figure 5. Proposed eco-friendly alternatives to nano- or micro-sized photocatalysts to treat OMWW.

6.1. Eco-Friendly Materials Used to Treat "Model Pollutants"

Several materials have already been investigated for the degradation of "model pollutants". They show promise for treating OMWW efficiently, and the scientific community could draw inspiration for appropriate evaluations. By way of example, magnetic bismuth-based photocatalysts have been largely used in the wastewater remediation field, and they could also find successful application in OMMW treatment, on which only preliminary studies have been reported.

In general, magnetic bismuth-based materials can be classified as magnetic bismuth-based oxyacid salt, magnetic oxyhalides, magnetic sulfides, and magnetic oxides.

Bismuth-based oxyacid salts (commonly labeled as Bi_aAO_b) have gained attention for their excellent visible-light absorption, band potential, and interesting chemical stability [165]. Their specific crystal phase confers good electron transport ability [166]. The introduction of proper magnetic components makes them easily recoverable and reusable for real applications.

In more detail, bismuth ferrite materials ($BiFeO_3$) are characterized by ferroelectricity and ferromagnetic features [167]. They have been explored as nanofibers [168], nanoparticles [169–171], nanosheets [172], nanotubes [173], microspheres [174], and nanorods [175], exploiting their magnetic properties and the 2.2 eV bandgap. Li et al. [173] compared the photocatalytic behaviour of $BiFeO_3$ in the form of nanoparticles, nanofibers, and hollow nanotubes, discovering the superior photoactivity of the latter due to the ultra-thin wall thickness and unique material structure. $BiFeO_3$ nanosheets of 140–230 nm side length and 30 nm thickness were synthesized by Zhu et al. [172] by hydrothermal procedures, demonstrating their high capability to degrade 89% rhodamine B (RhB) under 180 min of visible light irradiation. Bharathkumar et al. [176] prepared $BiFeO_3$ mat and mesh nanostructure materials by an electrospinning method, discovering that the photocatalytic degradation of the mesh sample was greater than that of the mat sample, probably due to the decrease of band gap energy. However, a limitation of the photocatalytic activity of $BiFeO_3$ is related to the fast photogenerated electron-hole recombination. In this context,

some studies pointed out that metal deposition and doping have a positive effect, reducing the charge recombination and improving their resulting photocatalytic performance [177].

Other bismuth-based oxyacid salts with narrow band gaps exist, such as $BiVO_4$ (2.26–2.51 eV), Bi_2WO_6 (2.56–2.92 eV), Bi_2MoO_6 (2.49–2.66 eV), and $Bi_2O_2CO_3$ (2.8–3.4 eV), which can be combined with magnetic components to obtain interesting and advanced materials with enhanced photocatalytic activity [178,179]. By way of example, Cam et al. introduced $MnFe_2O_4$ on $BiVO_4$, obtaining an innovative material with good photocatalytic activity and magnetic recovery [180]. Sakhare et al. [181] produced $BiVO_4/NiFe_2O_4$ composites able to degrade 98% methylene blue in 240 min of collected sunlight illumination and to maintain excellent stability even after four cycles. Bastami et al. [182] prepared magnetic Fe_3O_4/Bi_2WO_6 nanohybrids to degrade ibuprofen under solar light. Xiu et al. [183] developed 3D magnetic $Fe_3O_4/Ag/Bi_2MoO_6$ spheres, obtaining an advanced photocatalytic-Fenton coupling system, which exhibited excellent photocatalytic behaviors in the Aatrex degradation.

Bismuth oxyhalides (BiOX, X = Br, Cl, I) represent another family of bismuth-based materials, which have recently attracted scientific research due to their band gap, high stability, and non-toxicity [184,185]. They exhibit a tetragonal matlockite structure interlaced with $[Bi_2O_2]^{2+}$ flat plates and double halogen atomic layers, which reduce the electron-hole pairs' recombination, producing good photocatalytic behaviour [186,187]. In this context, the combination of BiOX and magnetic components represents an interesting perspective to obtain easily recoverable photocatalytic compounds on which many researchers are working. Briefly, Cao et al. [188] investigated the performances of $BiOBr/Fe_3O_4$ composites, prepared by solvothermal method, under visible light irradiation to degrade glyphosate. Li et al. [189] produced $BiOBr/NiFe_2O_4$ materials of different mass ratios according to a conventional hydrothermal approach, and their photocatalytic performances were explored in the photodegradation of methylene blue and phenol. The authors additionally synthesized BiOBr nanosheets decorated with $NiFe_2O_4$ nanoparticles and tested the samples in the rhodamine-B photodegradation [190], observing that the $BiOBr/NiFe_2O_4$10 (having 10 wt.% $NiFe_2O_4$) composite was able to degrade rhodamine-B more efficiently than the pure BiOBr and $NiFe_2O_4$ (99.8% rhodamine-B degradation after 30 min radiation). Sin et al. [191] prepared $N-BiOBr/NiFe_2O_4$ composites by a hydrothermal strategy, demonstrating the enhanced photocatalytic behaviour towards phenol and Cr(VI) removal.

Moreover, systems based on BiOCl and BiOI were additionally developed, and their photocatalytic performances have been properly investigated. In particular, Ma et al. [192] prepared magnetic $BiOCl/ZnFe_2O_4$ samples, showing their high photocatalytic activity towards penicillin-G degradation (99% penicillin-G degradation within 180 min under visible-light irradiation). Zhou et al. [193] studied ternary magnetic $Ag_2WO_4/BiOI/CoFe_2O_4$ hybrid compounds, evaluating their photocatalytic activity towards toxic elemental mercury Hg(0) removal. In addition, $BiOI/CoFe_2O_4$ composites modified with $AgIO_3$ [194] and Ag_2CO_3 [195] were found to be highly efficient in the photocatalytic reduction of Hg(0).

Finally, magnetic sulfides and oxides deserve to be also mentioned. The former (labeled as Bi_2S_3) is described by the 1.3 eV energy bandgap and complete visible light region response [196]. They can be combined with materials with magnetic features to promote charge separation and guarantee good recyclability. For example, Li et al. explored the potentialities of $Fe_3O_4/Bi_2S_3/BiOBr$ samples in the photodegradation of diclofenac and ibuprofen, observing *ca.* 94 and 97% conversion of the studied pollutants, respectively, after 40 and 30 min under visible light irradiation [197]. On the other hand, Zhu et al. tested Fe_3O_4/Bi_2S_3 microspheres towards Congo red removal, discovering good stability for continuous tests. The latter (commonly named Bi_2O_3) is an attractive material possessing high redox reversibility, bandgap spanning from 2.6 to 2.8 eV, and good electrochemical stability [198]. Several researchers combined it with magnetic compounds to obtain final easily recoverable materials. In particular, Abbasi et al. prepared 3D flower-like $Fe_3O_4@Bi_2O_3/g-C_3N_4$ nanocomposites, successively evaluating their photocatalytic activity towards indigo carmine degradation [199]. In this case, introducing the conductive

C layer in the nanocomposite sample could improve the photocatalytic behaviour. In addition, Gao et al. first obtained a C/Fe_3O_4 composite and then a double conductive $C/Fe_3O_4/Bi_2O_3$ photocatalyst. In this case, electron-hole pairs' recombination and the reverse electron transfer to Bi_2O_3 can be prevented [200].

6.2. Other Emerging Eco-Friendly Materials (Floating Devices, Membranes)

Due to their floating properties and good visible light utilization, floating photocatalysts could be considered an excellent choice to gradually substitute conventional photocatalysts [201]. In fact, since 1993, floating TiO_2-based materials have been studied [202]. In general, a floating device exploits a lightweight material to float on the water surface, and the photocatalytic performances are maximized thanks to its exposed large surface [203,204]. At the same time, due to its peculiar structure, it minimizes photocatalyst loss, avoiding the long-term contact between photocatalyst and pollutants, which can decrease photocatalytic activity. In the last decades, various supports (i.e., perlite, vermiculite, glass, cork, graphite, polymer) have been investigated as candidates for developing efficient floating photocatalysts [201].

Among them, by way of example, some of the authors studied the performance of aerogel water-floating based materials prepared by poly (vinyl alcohol) and polyvinylidene fluoride as a polymer platform and loaded with different semiconductors, such as g-C_3N_4, MoO_3, Bi_2O_3, Fe_2O_3 or WO_3, obtaining interesting results towards the reduction of Cr(VI) under visible light [204]. Moreover, Wang et al. [205] recently investigated the use of advanced spongy foam photocatalysts composed of BiOX compounds deposited onto polyurethane foams to degrade targeted pollutants, such as methyl orange, phenol, and chlortetracycline. These systems showed a high potential because they can conjugate high stability, excellent adaptability, and easy recovery, with high photocatalytic performances and good reusability.

In the present panorama, the possibility of using supports characterized by eco-friendly features (i.e., low-cost, non-toxicity, bioavailability) is a priority for further evaluation, and will require strenuous investigation efforts. Some researchers have already considered luffa cylindrica, alginate sphere, or light expanded clay aggregate (LECA), but their potentialities are still the object of study today. Following this perspective, Chawla et al. immobilized $MoSe_2/BiVO_4$ on luffa cylindrica, and then they tested it in phenol degradation, observing up to 97% removal within 2 h of visible light irradiation [206]. Huang et al. recently investigated the possibility of combining alginate spheres with magnetic components, finding exciting results. In this case, the excellent floating performance, together with the availability of reaction sites offered by the material, resulted in the degradation of the selected pollutants (e.g., methyl orange) [207].

Finally, the use of membranes deserves also to be cited. This technology has been investigated in the OMWW treatments for several advantages (simplicity, modulability, easy maintenance, high separation efficiency, small footprint, and easy scale-up) [208]. Several membrane types have been developed and produced, from the polymeric-based ones [209,210] to the inorganic-based ones [211]. All of them have shown excellent performance in the separation of targeted pollutants. However, membrane technology is characterized by some drawbacks. By way of examples, they may be limited by the high concentration of suspended solids present in the OMWW to be treated, and they suffer from foulant deposition due to contaminants separated from the feed. Thus, further treatments are usually required. In this context, Dzinun et al. [212–214] tried to develop a photocatalytic membrane to overcome the membrane fouling and use it as support for photocatalysts. In this case, the photocatalyst addition should minimize the fouling rate. Unfortunately, photocatalytic membranes are also affected by some drawbacks. For example, prolonged exposure to irradiation may ruin their structure, causing damage to the active surface area, which strongly impacts the photocatalytic efficiency [215]. In this context, many ideas are currently put into action by several researchers, as recently reported by Salim et al. [216,217].

All these interesting and promising results obtained in the decontamination of targeted pollutants present in wastewater can be a starting point to investigate more in detail what happens in the case of such complex matrices as OMWW.

7. Conclusions

This review provides a critical insight into the current status and the consequent advances related to OMWW treatments, underlying their potentialities and drawbacks. A particular focus on developing innovative eco-friendly photocatalysts, which could become valid alternatives to conventional systems, if properly optimized, is provided.

Nowadays, the OMWW sector plays a fundamental role in the European economy, but at the same time, it also leads to dramatic consequences on the environment and human health. In this context, the current challenge involves optimizing well-known and conventional technologies. Still, the most captivating challenge is the development of innovative advanced strategies, such as those based on photocatalysis. These latter offer many advantages (i.e., high efficiency, low cost) but require the use of novel materials to overcome the common issues related to using slurry reactors and difficult photocatalyst recovery.

In this scenario, the potential use of easily recoverable magnetic compounds as well as floating- and membrane-based devices points to new horizons for sustainability, alternative to conventional TiO_2-based systems. The application of these advanced systems still needs hard work by the research world. Their future success in real applications will create a bridge between environmental protection and a circular economy.

References

1. Ducom, G.; Gautier, M.; Pietraccini, M.; Tagutchou, J.P.; Lebouil, D.; Gourdon, M. Comparative analyses of three olive mill solid residues from different countries and processes for energy recovery by gasification. *Renew. Energy* **2020**, *145*, 180–189. [CrossRef]
2. Inglezakis, V.J.; Moreno, J.L.; Doula, M. Olive oil waste management EU Legislation: Current situation and policy recommendations. *Int. J. Chem. Environ. Eng. Syst.* **2012**, *3*, 65–77.
3. Mercé Sole, M.; Pons, L.; Conde, M.; Gaidau, C.; Baccardit, A. Characterization of Wet Olive Pomace Waste as Bio Based Resource for Leather Tanning. *Materials* **2021**, *14*, 5790. [CrossRef] [PubMed]
4. Kapellakis, I.E.; Tsagarakis, K.P.; Crowther, J.C. Olive oil history, production and by-product management. *Rev. Environ. Sci. Bio/Technol.* **2008**, *7*, 1–26. [CrossRef]
5. Azaizeh, H.; Abu Tayeh, H.N.; Gerchman, Y. Chapter 2: Valorisation of olive oil indus-try solid waste and production of ethanol and high value-added biomolecules. In *Biovalorisation of Wastes to Renewable Chemicals and Biofuels*; Elsevier: Amsterdam, The Netherlands, 2019; pp. 27–40. ISBN 9780128179512.
6. Paredes, C.; Cegarra, J.; Roig, A.; Sanchez-Monedero, M.A.; Bernal, M.P. Characterisation of olive mill wastewater (alpechin) and its sludge for agricultural purposes. *Bioresour. Technol.* **1999**, *67*, 111–115. [CrossRef]
7. Paraskeva, P.; Diamadopoulos, E. Technologies for olive mill wastewater (OMW) treatment: A review. *J. Chem. Technol. Biotechnol.* **2006**, *81*, 1475–1485. [CrossRef]
8. Potoglou, D.; Kouzeli-Katsiri, A.; Haralambopoulos, D. Solar distillation of olive mill wastewater. *Renew. Energy* **2004**, *29*, 569–579. [CrossRef]

9. Niaounakis, M.; Halvadakis, C.P. *Olive-Mill Waste Management—Literature Review and Patent Survey*; Typothito-George Dardanos: Athens, Greece, 2004.

10. Caputo, A.C.; Scacchia, F.; Pelagagge, P.M. Disposal of byproducts in olive oil industry: Waste-to-energy solutions. *Appl. Therm. Eng.* **2003**, *23*, 197–214. [CrossRef]

11. Al-Malah, K.; Azzam, M.O.J.; Abulail, N.I. Olive mills effluent (OME) wastewater post-treatment using activated clay. *Sep. Purif. Technol.* **2000**, *20*, 225–234. [CrossRef]

12. Azzam, M.O.J.; Al-Malah, K.I.; Abu-Lail, N.I. Dynamic posttreatment response of olive mill effluent wastewater using activated carbon. *J. Environ. Sci. Health A* **2004**, *39*, 269–280. [CrossRef]

13. Arvaniti, E.C.; Zagklis, D.P.; Papadakis, V.G.; Paraskeva, C.A. High-added value materials production from OMW: A technical and economical optimization. *Int. J. Chem. Eng.* **2012**, *2012*, 607219. [CrossRef]

14. Djellabi, R.; Giannantonio, R.; Falletta, E.; Bianchi, C.L. SWOT analysis of photocatalytic materials towards large scale environmental remediation. *Curr. Opin. Chem. Eng.* **2021**, *33*, 100696. [CrossRef]

15. Galloni, M.G.; Cerrato, G.; Giordana, A.; Falletta, E.; Bianchi, C.L. Sustainable Solar Light Photodegradation of Diclofenac by Nano- and Micro-Sized $SrTiO_3$. *Catalysts* **2022**, *12*, 804. [CrossRef]

16. Lucas, M.S.; Peres, J.A. Removal of COD from olive mill wastewater by Fenton's reagent: Kinetic study. *J. Hazard. Mater.* **2009**, *168*, 1253–1259. [CrossRef] [PubMed]

17. Stoller, M.; Bravi, M. Critical flux analyses on differently pretreated olive vegetation wastewater streams: Some case studies. *Desalination* **2010**, *250*, 578–582. [CrossRef]

18. Papaphilippou, P.C.; Yiannapas, C.; Politi, M.; Daskalaki, V.M.; Michael, C.; Kalogerakis, N.; Mantzavinos, D.; Fatta-Kassinos, D. Sequential coagulation–flocculation, solvent extraction and photo-Fenton oxidation for the valorization and treatment of olive mill effluent. *Chem. Eng. J.* **2013**, *224*, 82–88. [CrossRef]

19. Aziz, K.H.H.; Omer, K.M.; Mahyar, A.; Miessner, H.; Mueller, S.; Moeller, D. Applica-tion of Photocatalytic Falling Film Reactor to Elucidate the Degradation Pathways of Pharmaceutical Diclofenac and Ibuprofen in Aqueous Solutions. *Coatings* **2019**, *9*, 465. [CrossRef]

20. Aziz, K.H.H. Application of different advanced oxidation processes for the removal of chloroacetic acids using a planar falling film reactor. *Chemosphere* **2019**, *228*, 377–383. [CrossRef]

21. Podgornik, M.; Bucar-Miklavcic, M.; Levart, A.; Salobir, J.; Rezar, V.; Butinar, B. Chemical Characteristics of Two-Phase Olive-Mill Waste and Evaluation of Their Direct Soil Application in Humid Mediterranean Regions. *Agronomy* **2022**, *12*, 1621. [CrossRef]

22. Directive 2008/98/EC of the European Parliament and of the Council of 19 November 2008 on Waste and Repealing Certain Directives. Available online: https://eur-lex.europa.eu/legal-content/EN/TXT/?uri=celex%3A32008L0098 (accessed on 15 July 2022).

23. Council Directive 1999/31/EC on the Landfill of Waste. Available online: https://eur-lex.europa.eu/legal-content/EN/TXT/PDF/?uri=CELEX:01999L0031-20180704&from=FI (accessed on 10 July 2022).

24. Taccogna, G. *The Legal Regime of Olive Pomace Deriving from Olive Oil Extraction at Olive Mills, Waste, By-Products and Biomass*; On behalf of ARE S.p.A. Agenzia regionale per l'energia della Liguria, member of the community project: "MORE: Market of Olive Residues for Energy"; Department of Public and Procedural Law, University of Genoa: Genoa, Italy, 2010.

25. EC-DG. Survey of Wastes Spread on Land, Final Report, European Commission, Directorate-General for Environment. 2001. Available online: https://ec.europa.eu/environment/pdf/waste/compost/econanalysis_finalreport.pdf (accessed on 30 June 2022).

26. Aydar, A.Y.; Bagdatlioglu, N.; Köseoglu, O. Effect of ultrasound on olive oil extraction and optimization of ultrasound-assisted extraction of extra virgin olive oil by response surface methodology (RSM). *Grasas Aceites* **2017**, *68*, e189. [CrossRef]

27. Arvanitoyannis, I.S.; Kassaveti, A.; Stefanatos, S. Olive Oil Waste Treatment: A Comparative and Critical Presentation of Methods, Advantages & Disadvantages. *Crit. Rev. Food Sci. Nutr.* **2007**, *47*, 187–229. [PubMed]

28. Facts and Definitions: The Olive Oil Source. Available online: http://www.oliveoilsource.com/millandpressfacts.htm (accessed on 25 June 2022).

29. Olive Oil Waste Treatment. Available online: http://www.ucm.es/info/improliv/allgem.htm (accessed on 25 June 2022).

30. Dakhli, R.D. Agronomic Application of Olive Mill Waste Water: Short-Term Effect on Soil Chemical Properties and Barley Performance Under Semiarid Mediterranean Conditions. *EQA-Int. J. Environ. Qual.* **2018**, *27*, 1–17.

31. Fedeli, E.; Camurati, F. Valorisation des margines et des grignons´epuises par recuperation de quelques composants. In Proceedings of the Seminaire International sur la Valorisation des Sous-Produits de L'olivier PNUD/FAO/COI, Monastir, Tunisia, 15–17 December 1981.

32. Rocha, C.; Soria, M.A.; Madeira, L.M. Olive Mill Wastewater Valorization through Steam Reforming Using Multifunctional Reactors: Challenges of the Process Intensification. *Energies* **2022**, *15*, 920. [CrossRef]

33. Production of Olive Oil. Available online: http://www.oliveoilsource.com/millandpressfacts3.htm (accessed on 26 June 2022).

34. Abenoza, M.; Benito, M.; Saldaña, G.; Alvarez, I.; Raso, J.; Sanchez-Gimeno, A.C. Effects of pulsed electric field on yield extrac-tion and quality of olive oil. *Food Bioprocess Technol.* **2013**, *6*, 1367–1373. [CrossRef]

35. Puértolas, E.; Martínez de Marañón, I. Olive oil pilot-production assisted by pulsed electric field: Impact on extraction yield, chemical parameters and sensory properties. *Food Chem.* **2015**, *167*, 497–502. [CrossRef] [PubMed]

36. Clodoveo, M.L.; Durante, V.; La Notte, D. Working towards the development of innovative ultrasound equipment for the extraction of virgin olive oil. *Ultrason. Sonochem.* **2013**, *20*, 1261–1270. [CrossRef]

37. Aydar, A.Y. *Utilization of Response Surface Methodology in Optimization of Extraction of Plant Materials*; Intech Open: London, UK, 2018; pp. 157–169.

38. Meroni, D.; Djellabi, R.; Ashokkumar, M.; Bianchi, C.L.; Boffito, D.C. Sonoprocessing: From Concepts to Large-Scale Reactors. *Chem. Rev.* **2022**, *122*, 3219–3258. [CrossRef] [PubMed]

39. Bermúdez-Aguirre, D.; Mobbs, T.; Barbosa-cánovas, G.V. *Ultrasound Technologies for Food and Bioprocessing*; Epub ahead of print; Springer: Berlin/Heidelberg, Germany, 2011. [CrossRef]

40. Chemat, F.; Zill-E-Huma, R.; Khan, M.K. Applications of ultrasound in food technology: Processing, preservation and extraction. *Ultrason. Sonochem.* **2011**, *18*, 813–835. [CrossRef] [PubMed]

41. Veneziani, G.; Sordini, B.; Taticchi, A.; Esposto, S.; Selvaggini, R.; Urbani, S.; Di Maio, I.; Servili, M. Improvement of Olive Oil Mechanical Extraction: New Technologies, Process Efficiency, and Extra Virgin Olive Oil Quality. In *Products from Olive Tree Dimitrios Boskou and Maria Lisa Clodoveo*; Intech Open: London, UK, 2016; Available online: https://www.intechopen.com/books/products-from-olive-tree/improvement-of-olive-oil-mechanicalextraction-new-technologies-processefficiency-and-extra-virgin (accessed on 20 June 2022). [CrossRef]

42. Clodoveo, M.L. An overview of emerging techniques in virgin olive oil extraction process: Strategies in the development of innovative plants. *J. Agric. Eng.* **2013**, *44*, 49–59. [CrossRef]

43. Clodoveo, M.L. New advances in the development of innovative virgin olive oil extraction plants: Looking back to see the future. *Food Res. Int.* **2013**, *54*, 726–729. [CrossRef]

44. Clodoveo, M.L.; Hachicha Hbaieb, R. Beyond the traditional virgin olive oil extraction systems: Searching innovative and sustainable plant engineering solutions. *Food Res. Int.* **2013**, *54*, 1926–1933. [CrossRef]

45. Clodoveo, M.L.; Camposeo, S.; Amirante, R.; Dugo, G.; Cicero, N.; Boskou, D. Research and Innovative Ap-proaches to Obtain Virgin Olive Oils with a Higher Level of Bioactive Constituents. *Olive Olive Oil Bioact. Const.* **2015**, *7*, 179–215. [CrossRef]

46. Sun, D.W. *Emerging Technologies for Food Processing*, 2nd ed.; Elsevier Inc.: Dublin, Ireland, 2014.

47. Çavdar, H.K.; Yanık, D.K.; Gök, U.; Gogus, F. Optimisation of microwave-assisted extraction of pomegranate (*Punica granatum* L.) seed oil and evaluation of Its physicochemical and bioactive properties. *Food Technol. Biotechnol.* **2017**, *55*, 86–94. [PubMed]

48. Aydar, A.Y. Chapter: Emerging extraction technologies in olive oil production. In *Technological Innovation in the Olive Oil Production Chain*; Intech Open: London, UK, 2018. [CrossRef]

49. Jiménez, A.; Beltrán, G.; Uceda, M. High-power ultra-sound in olive paste pretreatment. Effect on process yield and virgin olive oil characteristics. *Ultrason. Sonochem.* **2007**, *14*, 725–731. [CrossRef] [PubMed]

50. Bejaoui, M.A.; Beltrán, G.; Sánchez-Ortiz, A.; Sanchez, S.; Jimenez, A. Continuous high power ultrasound treatment before malaxation, a laboratory scale approach: Effect on virgin olive oil quality criteria and yield. *Eur. J. Lipid Sci. Technol.* **2016**, *118*, 332–336. [CrossRef]

51. Aydar, A.Y. Physicochemical characteristics of extra virgin olive oils obtained by ultrasound assisted extraction from different olive cultivars. *Int. J. Sci. Technol. Res.* **2018**, *4*, 1–10.

52. Bejaoui, M.A.; Beltran, G.; Aguilera, M.P.; Jimenez, A. Continuous conditioning of olive paste by high power ultrasounds: Response surface methodology to predict temperature and its effect on oil yield and virgin olive oil characteristics. *LWT-Food Sci. Technol.* **2016**, *69*, 175–184. [CrossRef]

53. Kadi, H.; Moussaoui, R.; Djadoun, S.; Sharrock, P. Microwave assisted extraction of olive oil pomace by acidic hexane. *Iran. J. Chem. Chem. Eng.* **2016**, *35*, 73–79.

54. Leone, A.; Tamborrino, A.; Zagaria, R.; Sabella, E.; Romaniello, R. Plant innovation in the olive oil extraction process: A comparison of efficiency and energy consumption between microwave treatment and traditional malaxation of olive pastes. *J. Food Eng.* **2015**, *146*, 44–52. [CrossRef]

55. Clodoveo, M.L.; Paduano, A.; Di Palmo, T.; Crupi, P.; Corbo, F.; Pesce, V.; Distaso, E.; Tamburrano, P.; Amirante, R. Engineering design and prototype development of a full scale ultrasound system for virgin olive oil by means of numerical and experimental analysis. *Ultrason. Sonochem.* **2017**, *37*, 169–181. [CrossRef]

56. Leal, A.L.; Soria, M.A.; Madeira, L.M. Autothermal reforming of impure glycerol for H_2 production: Thermodynamic study including in situ CO_2 and/or H_2 separation. *Int. J. Hydrogen Energy* **2016**, *41*, 2607–2620. [CrossRef]

57. Agency, I.E. Hydrogen. 2021. Available online: https://www.iea.org/reports/hydrogen (accessed on 12 August 2022).

58. Agency, I.E. Global Hydrogen Demand by Sector in the Net Zero Scenario, 2020–2030. 2021. Available online: https://www.iea.org/data-and-statistics/charts/global-hydrogen-demand-by-sector-in-the-net-zero-scenario-2020-2030 (accessed on 12 August 2022).

59. Kapellakis, I.E.; Tsagarakis, K.P.; Avramaki, C.; Angelakis, A.N. Olive mill wastewater management in river basins: A case study in Greece. *Agric. Water Manag.* **2006**, *82*, 354–370. [CrossRef]

60. Chartzoulakis, K.; Psarras, G.; Moutsopoulou, M.; Stefanoudaki, E. Application of olive mill wastewater to a Cretan olive orchard: Effects on soil properties, plant performance and the environment. *Agric. Ecosyst. Environ.* **2010**, *138*, 293–298. [CrossRef]

61. Watanabe, K. Microorganisms relevant to bioremediation. *Curr. Opin. Biotechnol.* **2001**, *12*, 237–241. [CrossRef]

62. Enhanced Bioremediation. Available online: http://www.cpeo.org/techtree/ttdescript/ensolmx.htm (accessed on 15 June 2022).

63. Ehaliotis, C.; Papadopoulou, K.; Kotsou, M.; Mari, I.; Balis, C. Adaptation and population dynamics of Azotobacter vinelandii during aerobic biological treatment of olive-mill wastewater. *FEMS Microbiol. Ecol.* **1999**, *30*, 301–311. [CrossRef]

64. Di Gioia, D.; Barberio, C.; Spagnesi, S.; Marchetti, L.; Fava, F. Characterization of four olive-mill-wastewater indigenous bacterial strains capable of aerobically degrading hydroxylated and methoxylated monocyclic aromatic compounds. *Arch. Microbiol.* **2002**, *178*, 208–217. [CrossRef] [PubMed]

65. Di Gioia, D.; Bertin, L.; Fava, F.; Marchetti, L. Biodegradation of hydroxylated and methoxylated benzoic, phenylacetic and phenylpropenoic acids present in olive mill wastewaters by two bacterial strains. *Res. Microbiol.* **2001**, *152*, 83–93. [CrossRef]

66. Piperidou, C.I.; Chaidou, C.I.; Stalikas, C.D.; Soulti, K.; Pilidis, G.A.; Balis, C. Bioremediation of olive oil mill wastewater: Chemical alternations induced by Azotobacter vinelandii. *J. Agric. Food Chem.* **2000**, *48*, 1941–1948. [CrossRef]

67. Yesilada, O.; Sik, S.; Sam, M. Biodegradation of olive oil mill wastewater by Coriolus versicolor and Funalia trogii: Effects of agitation, initial COD concentration, inoculum size and immobilization. *World J. Microbiol. Biotechnol.* **1997**, *14*, 37–42. [CrossRef]

68. Zagklis, D.P.; Arvaniti, E.C.; Papadakis, V.G.; Paraskeva, C.A. Sustainability analysis and benchmarking of olive mill wastewater treatment methods. *J. Chem. Technol. Biotechnol.* **2013**, *88*, 742–750. [CrossRef]

69. Tomati, U.; Galli, E.; Fiorelli, F.; Pasetti, L. Fertilizers from composting of olive-mill wastewaters. *Int. Biodeterior. Biodegrad.* **1996**, *38*, 155–162. [CrossRef]

70. Hachicha, S.; Cegarra, J.; Sellami, F.; Hachicha, R.; Drira, N.; Medhioub, K.; Ammar, E. Elimination of polyphenols toxicity from olive mill wastewater sludge by its co-composting with sesame bark. *J. Hazard. Mater.* **2009**, *161*, 1131–1139. [CrossRef] [PubMed]

71. New Technologies for Husks and Waste Waters Recycling. Available online: https://webgate.ec.europa.eu/life/publicWebsite/project/details/1782 (accessed on 5 June 2022).

72. Gavala, H.N.; Skiadas, I.V.; Bozinis, N.A.; Lyberatos, G. Anaerobic codigestion of agricultural industries' wastewaters. *Water Sci. Technol.* **1996**, *34*, 67–75. [CrossRef]

73. Zouari, N.; Ellouz, R. Toxic effect of coloured olive compounds on the anaerobic digestion of olive oil mill effluent in UASB-like reactors. *J. Chem. Technol. Biotechnol.* **1996**, *66*, 414–420. [CrossRef]

74. Stamatelatou, K.; Kopsahelis, A.; Blika, P.S.; Paraskeva, C.A.; Lyberatos, G. Anaerobic digestion of olive mill wastewater in a periodic anaerobic baffled reactor (PABR) followed by further effluent purification via membrane separation technologies. *J. Chem. Technol. Biotechnol.* **2009**, *84*, 909–917. [CrossRef]

75. Boari, G.; Brunetti, A.; Passino, R.; Rozzi, A. Anaerobic digestion of olive oil mill wastewaters. *Agric. Wastes* **1984**, *10*, 161–175. [CrossRef]

76. Aktas, E.S.; Imre, S.; Ersoy, L. Characterization and lime treatment of olive mill wastewater. *Water Res.* **2001**, *35*, 2336–2340. [CrossRef]

77. Boukhoubza, F.; Jail, A.; Korchi, F.; Idrissi, L.L.; Hannache, H.; Duarte, J.C.; Hassani, L.; Nejmeddine, A. Application of lime and calcium hypochlorite in the dephenolisation and discolouration of olive mill wastewater. *J. Environ. Manag.* **2009**, *91*, 124–132. [CrossRef]

78. Saglık, S.; Ersoy, L.; Imre, S. Oil recovery from lime-treated wastewater of olive mills. *Eur. J. Lipid Sci. Technol.* **2002**, *104*, 212–215. [CrossRef]

79. Ugurlu, M.; Kula, I. Decolourization and removal of some organic compounds from olive mill wastewater by advanced oxidation processes and lime treatment. *Environ. Sci. Pollut. Res.* **2007**, *14*, 319–325. [CrossRef]

80. Inan, H.; Dimoglo, A.; Simsek, H.; Karpuzcu, M. Olive oil mill wastewater treatment by means of electro-coagulation. *Sep. Purif. Technol.* **2004**, *36*, 23–31. [CrossRef]

81. Israilides, C.J.; Vlyssides, A.G.; Mourafeti, V.N.; Karvouni, G. Olive oil wastewater treatment with the use of an electrolysis system. *Bioresour. Technol.* **1997**, *61*, 163–170. [CrossRef]

82. Giannis, A.; Kalaitzakis, M.; Diamadopoulos, E. Electrochemical treatment of olive mill wastewater. *J. Chem. Technol. Biotechnol.* **2007**, *82*, 663–671. [CrossRef]

83. Papastefanakis, N.; Mantzavinos, D.; Katsaounis, A. DSA electrochemical treatment of olive mill wastewater on Ti/RuO_2 anode. *J. Appl. Electrochem.* **2010**, *40*, 729–737. [CrossRef]

84. Chatzisymeon, E.; Dimou, A.; Mantzavinos, D.; Katsaounis, A. Electrochemical oxidation of model compounds and olive mill wastewater over DSA electrodes: 1. The case of Ti/IrO_2 anode. *J. Hazard. Mater.* **2009**, *167*, 268–274. [CrossRef]

85. Ahmed, B.; Limem, E.; Abdel-Wahab, A.; Nasr, B. Photo-Fenton treatment of actual agro-industrial wastewaters. *Ind. Eng. Chem. Res.* **2011**, *50*, 6673–6680. [CrossRef]

86. Aki, S.N.V.K.; Abraham, M.A. An economic evaluation of catalytic supercritical water oxidation: Comparison with alternative waste treatment technologies. *Environ. Prog.* **1998**, *17*, 246–255. [CrossRef]

87. Rivas, F.J.; Gimeno, O.; Portela, J.R.; de la Ossa, E.M.; Beltran, F.J. Supercritical water oxidation of olive oil mill wastewater. *Ind. Eng. Chem. Res.* **2001**, *17*, 246–255. [CrossRef]

88. Chatzisymeon, E.; Diamadopoulos, E.; Mantzavinos, D. Effect of key operating parameters on the non-catalytic wet oxidation of olive mill wastewaters. *Water Sci. Technol.* **2009**, *59*, 2509–2518. [CrossRef]

89. Weichgrebe, D.; Vogelpohl, A. A comparative study of wastewater treatment by chemical wet oxidation. *Chem. Eng. Process. Process. Intensif.* **1994**, *33*, 199–203. [CrossRef]

90. Katsoyiannis, I.A.; Canonica, S.; von Gunten, U. Efficiency and energy requirements for the transformation of organic micropollutants by ozone, O_3/H_2O_2 and UV/H_2O_2. *Water Res.* **2011**, *45*, 3811–3822. [CrossRef] [PubMed]

91. Karageorgos, P.; Coz, A.; Charalabaki, M.; Kalogerakis, N.; Xekoukoulotakis, N.P.; Mantzavinos, D. Ozonation of weathered olive mill wastewaters. *J. Chem. Technol. Biotechnol.* **2006**, *81*, 1570–1576. [CrossRef]

92. Mousavi, M.; Habibi-Yangjeh, A.; Pouran, S.R. Review on magnetically separable graphitic carbon nitride-based nanocomposites as promising visible-light-driven photocatalysts. *J. Mater. Sci. Mater. Electron.* **2018**, *29*, 1719–1747. [CrossRef]

93. Shekofteh-Gohari, M.; Habibi-Yangjeh, A.; Abitorabi, M.; Rouhi, A. Magnetically separable nanocomposites based on ZnO and their applications in photocatalytic processes: A review. *Crit. Rev. Environ. Sci. Technol.* **2018**, *48*, 806–857. [CrossRef]

94. Djellabi, R.; Noureen, L.; Dao, V.D.; Meroni, D.; Falletta, E.; Dionysiou, D.D.; Bianchi, C.L. Recent advances and challenges of emerging solar-driven steam and the contribution of photocatalytic effect. *Chem. Eng. J.* **2022**, *431*, 134024. [CrossRef]

95. Pirhashemi, M.; Habibi-Yangjeh, A.; Rahim Pouran, S. Review on the criteria anticipated for the fabrication of highly efficient ZnO-based visible-light-driven photo-catalysts. *J. Ind. Eng. Chem.* **2018**, *62*, 1–25. [CrossRef]

96. Ahmad, R.; Ahmad, Z.; Khan, A.U.; Mastoi, N.R.; Aslam, M.; Kim, J. Photocatalytic systems as an advanced environmental remediation: Recent developments, limitations and new avenues for applications. *J. Environ. Chem. Eng.* **2016**, *4*, 4143–4164. [CrossRef]

97. Tolosana-Moranchel, A.; Ovejero, D.; Barco, B.; Bahamonde, A.; Díaz, E.; Faraldos, M. An approach on the comparative behavior of chloro/nitro substituted phenols photocatalytic degradation in water. *J. Environ. Chem. Eng.* **2019**, *7*, 103051. [CrossRef]

98. Chatzisymeon, E.; Xekoukoulotakis, N.P.; Mantzavinos, D. Determination of key operating conditions for the photocatalytic treatment of olive mill wastewaters. *Catal. Today* **2009**, *144*, 143–148. [CrossRef]

99. Justino, C.I.; Duarte, K.; Loureiro, F.; Pereira, R.; Antunes, S.C.; Marques, S.M.; Gonçalves, F.; Rocha-Santos, T.A.P.; Freitas, A.C. Toxicity and organic content characterization of olive oil mill wastewater undergoing a sequential treatment with fungi and photo-Fenton oxidation. *J. Hazard. Mater.* **2009**, *172*, 1560–1572. [CrossRef]

100. Ochando-Pulido, J.M.; Hodaifa, G.; Víctor-Ortega, M.D.; Martínez-Férez, A. A novel photocatalyst with ferromagnetic core used for the treatment of olive oil mill effluents from two-phase production process. *Sci. World J.* **2013**, *2013*, 196470. [CrossRef] [PubMed]

101. Lafi, W.K.; Shannak, B.; Al-Shannag, M.; Al-Anber, Z.; Al-Hasan, M. Treatment of olive mill wastewater by combined advanced oxidation and biodegradation. *Sep. Purif. Technol.* **2009**, *70*, 141–146. [CrossRef]

102. Ochando-Pulido, J.M.; Stoller, M. Kinetics and boundary flux optimization of integrated photocatalysis and ultrafiltration process for two-phase vegetation and olive washing wastewaters treatment. *Chem. Eng. J.* **2015**, *279*, 387–395. [CrossRef]

103. Costa, J.C.; Alves, M.M. Posttreatment of olive mill wastewater by immobilized TiO_2 photocatalysis. *Photochem. Photobiol.* **2013**, *89*, 545–551. [CrossRef]

104. Ruzmanova, Y.; Stoller, M.; Chianese, A. Photocatalytic treatment of olive mill wastewater by magnetic core titanium dioxide nanoparticles. *Chem. Eng. Trans.* **2013**, *32*, 2269–2274.

105. Gernjak, W.; Maldonado, M.I.; Malato, S.; Cáceres, J.; Krutzler, T.; Glaser, A.; Bauer, R. Pilot-plant treatment of olive mill wastewater (OMW) by solar TiO_2 photocatalysis and solar photo-Fenton. *Sol. Energy* **2004**, *77*, 567–572. [CrossRef]

106. Fujishima, A.; Honda, K. Electrochemical photolysis of water at a semiconductor electrode. *Nature* **1972**, *238*, 37–38. [CrossRef] [PubMed]

107. Xing, Z.; Zhang, J.; Cui, J.; Yin, J.; Zhao, T.; Kuang, J.; Xiu, Z.; Wan, N.; Zhou, W. Recent advances in floating TiO_2-based photocatalysts for environmental application. *Appl. Catal. B Environ.* **2018**, *225*, 452–467. [CrossRef]

108. Zhao, Y.; Wang, Y.; Xiao, G.; Su, H. Fabrication of biomaterial/TiO_2 composite photocatalysts for the selective removal of trace environmental pollutants. *Chin. J. Chem. Eng.* **2019**, *27*, 1416–1428. [CrossRef]

109. Tomar, L.J.; Chakrabarty, B.S. Synthesis, structural and optical properties of TiO_2-ZrO_2 nanocomposite by hydrothermal method. *Adv. Mater. Lett.* **2013**, *4*, 64–67. [CrossRef]

110. Habibi-Yangjeh, A.; Feizpoor, S.; Seifzadeh, D.; Ghosh, S. Improving visible-light-induced photocatalytic ability of TiO_2 through coupling with Bi_3O_4Cl and carbon dot nanoparticles. *Sep. Purif. Technol.* **2020**, *238*, 116404. [CrossRef]

111. Feizpoor, S.; Habibi-Yangjeh, A.; Yubuta, K. Integration of carbon dots and polyaniline with TiO_2 nanoparticles: Substantially enhanced photocatalytic activity to removal various pollutants under visible light. *J. Photochem. Photobiol. A Chem.* **2018**, *367*, 94–104. [CrossRef]

112. Divya, K.S.; Madhu, A.K.; Umadevi, T.U.; Suprabha, T.; Nair, P.R.; Suresh, M. Improving the photocatalytic performance of TiO_2 via hybridizing with graphene. *J. Semicond.* **2017**, *38*, 063002. [CrossRef]

113. Kubiak, A.; Siwinska-Ciesielczyk, K.; Jesionowski, T. Titania-based hybrid materials with ZnO, ZrO_2 and MoS_2: A review. *Materials* **2018**, *11*, 2295. [CrossRef]

114. Shao, G.N.; Imran, S.M.; Jeon, S.J.; Engole, M.; Abbas, N.; Salman Haider, M.; Kang, S.J.; Kim, H.T. Sol–gel synthesis of photoactive zirconia–titania from metal salts and investigation of their photocatalytic properties in the photodegradation of methylene blue. *Powder Technol.* **2014**, *258*, 99–109. [CrossRef]

115. Chen, Q.; Wei, W.; Tang, J.; Lin, J.; Li, S.; Zhu, M. Dopamine-assisted preparation of Fe_3O_4@MnO_2 yolk@shell microspheres for improved pseudocapacitive performance. *Electrochim. Acta* **2019**, *317*, 628–637. [CrossRef]

116. Karafas, E.S.; Romanias, M.N.; Stefanopoulos, V.; Binas, V.; Zachopoulos, A.; Kiriakidis, G.; Papagiannakopoulos, P. Effect of metal doped and co-doped TiO_2 photocatalysts oriented to degrade indoor/outdoor pollutants for air quality improvement. A kinetic and product study using acetaldehyde as probe molecule. *J. Photochem. Photobiol. A Chem.* **2019**, *371*, 255–263. [CrossRef]

117. Mokoena, T.P.; Tshabalala, Z.P.; Hillie, K.T.; Swart, H.C.; Motaung, D.E. The blue luminescence of p-type NiO nanostructured material induced by defects: H_2S gas sensing characteristics at a relatively low operating temperature. *Appl. Surf. Sci.* **2020**, *525*, 146002. [CrossRef]

118. Li, J.; Chen, Y.; Wu, Q.; Wu, J.; Xu, Y. Synthesis of sea-urchin-like Fe_3O_4/SnO_2 heterostructures and its application for environmental remediation by removal of p-chlorophenol. *J. Mater. Sci.* **2018**, *54*, 1341–1350. [CrossRef]

119. Bhardwaj, N.; Satpati, B.; Mohapatra, S. Plasmon-enhanced photoluminescence from SnO_2 nanostructures decorated with Au nanoparticles. *Appl. Surf. Sci.* **2020**, *504*, 144381. [CrossRef]

120. Imran, M.; Riaz, S.; Sanaullah, I.; Khan, U.; Sabri, A.N.; Naseem, S. Microwave assisted synthesis and antimicrobial activity of Fe_3O_4-doped ZrO_2 nanoparticles. *Ceram. Int.* **2019**, *45*, 10106–10113. [CrossRef]

121. Khan, S.; Kim, J.; Sotto, A.; Van der Bruggen, B. Humic acid fouling in a submerged photocatalytic membrane reactor with binary TiO_2–ZrO_2 particles. *J. Ind. Eng. Chem.* **2015**, *21*, 779–786. [CrossRef]

122. Zhang, Y.; Wang, X.; Wang, C.; Zhai, H.; Liu, B.; Zhao, X.; Fang, D.; Wei, Y. Facile preparation of flexible and stable superhydrophobic non-woven fabric for efficient oily wastewater treatment. *Surf. Coat. Technol.* **2019**, *357*, 526–534. [CrossRef]

123. Elbasuney, S.; Elsayed, M.A.; Mostafa, S.F.; Khalil, W.F. MnO_2 nanoparticles supported on porous Al_2O_3 substrate for wastewater treatment: Synergy of adsorption, oxidation, and photocatalysis. *J. Inorg. Organomet. Polym. Mater.* **2019**, *29*, 827–840. [CrossRef]

124. Yaacob, N.; Sean, G.P.; Nazri, N.A.M.; Ismail, A.F.; Abidin, M.N.Z.; Subramaniam, M.N. Simultaneous oily wastewater adsorption and photodegradation by ZrO_2–TiO_2 heterojunction photocatalysts. *J. Water Process Eng.* **2021**, *39*, 101644. [CrossRef]

125. Skocaj, M.; Filipic, M.; Petkovic, J.; Novak, S. Titanium dioxide in our everyday life; is it safe? *Radiol. Oncol.* **2011**, *45*, 227–247. [CrossRef] [PubMed]

126. Sakthivel, S.; Neppolian, B.; Shankar, M.V.; Arabindoo, B.; Palanichamy, A.; Murugesan, V. Solar photocatalytic degradation of azodye: Comparison of photocatalytic efficiency of ZnO and TiO_2. *Sol. Energy Mater. Sol. Cells* **2003**, *77*, 65–82. [CrossRef]

127. Kobayakawa, K.; Sato, C.; Sato, Y.; Fujishima, A. Continuous-flow photoreactor packed with titanium dioxide immobilized on large silica gel beads to decompose oxalic acid in excess water. *J. Photochem. Photobiol. A Chem.* **1998**, *118*, 65–69. [CrossRef]

128. Kamat, P.V. Photochemistry on nonreactive and reactive (semiconductor) surfaces. *Chem. Rev.* **1993**, *93*, 267–300. [CrossRef]

129. Comparelli, R.; Fanizza, E.; Curri, M.L.; Cozzoli, P.D.; Mascolo, G.; Agostiano, A. UV-induced photocatalytic degradation of azo dyes by organic capped ZnO nanocrystals immobilized onto substrates. *Appl. Catal. B Environ.* **2005**, *62*, 1–11. [CrossRef]

130. Fouad, O.A.; Ismail, A.A.; Zaki, Z.I.; Mohamed, R.M. Zinc oxide thin films prepared by thermal evaporation deposition and its photocatalytic activity. *Appl. Catal. B Environ.* **2006**, *62*, 144–149. [CrossRef]

131. Yeber, M.C.; Rodriguez, J.; Freer, J.; Baeza, J.; Duran, N.H.; Mansilla, D. Advanced oxidation of a pulp mill bleaching wastewater. *Chemosphere* **1999**, *39*, 1679–1688. [CrossRef]

132. Khodja, A.A.; Sheili, T.; Pihichowski, J.F.; Boule, P. Photocatalytic degradation of 2-phenylphenol on TiO_2 and ZnO in aqueous suspensions. *J. Photochem. Photobiol. A* **2001**, *141*, 231–239. [CrossRef]

133. Serpone, N.; Maruthamuthu, P.; Pichat, P.; Pelizzetti, E.; Hidaka, H. Exploiting the interparticle electron transfer process in the photocatalyzed oxidation of phenol, 2-chlorophenol and pentachlorophenol chemical evidence for electron and hole transfer between coupled semiconductors. *J. Photochem. Photobiol. A Chem.* **2001**, *85*, 247–253. [CrossRef]

134. Sakthivel, S.; Shankar, M.V.; Palanichamy, M.; Arabindoo, B.; Murugesan, V. Photocatalytic decomposition of leather dye: Comparative study of TiO_2 supported on alumina and glass beads. *J. Photochem. Photobiol. A Chem.* **2002**, *148*, 153–159. [CrossRef]

135. Ochando-Pulido, J.M.; Pimentel-Moral, S.; Verardo, V.; Martinez-Ferez, A. A focus on advanced physico-chemical processes for olive mill wastewater treatment. *Sep. Purif. Technol.* **2017**, *179*, 161–174. [CrossRef]

136. Andreozzi, R.; Canterino, M.; Di Somma, I.; Lo Giudice, R.; Marotta, R.; Pinto, G.; Pollio, A. Effect of combined physico-chemical processes on the phytotoxicity of olive mill wastewaters. *Water Res.* **2008**, *42*, 1684–1692. [CrossRef] [PubMed]

137. Rizzo, L.; Lofrano, G.; Grassi, M.; Belgiorno, V. Pretreatment of olive mill wastewater by chitosan coagulation and advanced oxidation processes. *Sep. Purif. Technol.* **2008**, *63*, 648–653. [CrossRef]

138. Aytar, P.; Gedikli, S.; Sam, M.; Farizoglu, B.; Çabuk, A. Sequential treatment of olive oil mill wastewater with adsorption and biological and photo-Fenton oxidation. *Environ. Sci. Pollut. Res.* **2013**, *20*, 3060–3067. [CrossRef] [PubMed]

139. Hodaifa, G.; Agabo, C.; Moya, A.J.; Pacheco, R.; Mateo, S. Treatment of olive oil mill wastewater by UV-light and UV/H_2O_2 system. *Int. J. Green Technol.* **2015**, *1*, 46–53. [CrossRef]

140. Ruzmanova, Y.; Ustundas, M.; Stoller, M.; Chianese, A. Photocatalytic treatment of olive mill wastewater by N-doped titanium dioxide nanoparticles under visible light. *Chem. Eng. Trans.* **2013**, *32*, 2233–2238.

141. Cai, Q.; Zhu, Z.; Chen, B.; Zhang, B. Oil-in-water emulsion breaking marine bacteria for demulsifying oily wastewater. *Water Res.* **2019**, *149*, 292–301. [CrossRef] [PubMed]

142. Ahmad, T.; Guria, C.; Mandal, A. Synthesis, characterization and performance studies of mixed-matrix poly(vinyl chloride)-bentonite ultrafiltration membrane for the treatment of saline oily wastewater. *Process. Saf. Environ. Prot.* **2018**, *116*, 703–717. [CrossRef]

143. Perez-Calderon, J.; Santos, M.V.; Zaritzky, N. Optimal clarification of emulsified oily wastewater using a surfactant/chitosan biopolymer. *J. Environ. Chem. Eng.* **2018**, *6*, 3808–3818. [CrossRef]

144. Cebeci, M.S.; Gokçek, O.B. Investigation of the treatability of molasses and industrial oily wastewater mixture by an anaerobic membrane hybrid system. *J. Environ. Manag.* **2018**, *224*, 298–309. [CrossRef]

145. Elanchezhiyan, S.S.; Meenakshi, S. Encapsulation of metal ions between the biopolymeric layer beads for tunable action on oil particles adsorption from oily wastewater. *J. Mol. Liq.* **2018**, *255*, 429–438. [CrossRef]

146. Liu, B.; Chen, B.; Zhang, B. Oily wastewater treatment by nano-TiO_2-induced photocatalysis. *IEEE Nanotechnol.* **2017**, *11*, 2–13.

147. Yao, T.; Jia, W.; Feng, Y.; Zhang, J.; Lian, Y.; Wu, J.; Zhang, X. Preparation of reduced graphene oxide nanosheet/FexOy/nitrogen-doped carbon layer aerogel as pho-to-Fenton catalyst with enhanced degradation activity and reusability. *J. Hazard. Mater.* **2019**, *362*, 62–71. [CrossRef]

148. Rasheed, T.; Bilal, M.; Iqbal, H.M.N.; Hu, H.; Zhang, X. Reaction mechanism and degradation pathway of rhodamine 6G by photocatalytic treatment. *Water Air Soil Pollut.* **2017**, *228*, 291. [CrossRef]

149. Bilal, M.; Rasheed, T.; Iqbal, H.M.N.; Hu, H.; Wang, W.; Zhang, X. Toxicological assessment and UV/TiO_2-based induced degradation profile of reactive black 5 dye. *Environ. Manag.* **2018**, *61*, 171–180. [CrossRef]

150. Ma, M.; Yang, Y.; Chen, Y.; Jiang, J.; Ma, Y.; Wang, Z.; Huang, W.; Wang, S.; Liu, M.; Ma, D.; et al. Fabrication of hollow flower-like magnetic Fe_3O_4/C/MnO_2/C_3N_4 composite with enhanced photocatalytic activity. *Sci. Rep.* **2021**, *11*, 2597. [CrossRef] [PubMed]

151. Ma, M.; Yang, Y.; Chen, Y.; Ma, Y.; Lyu, P.; Cui, A.; Huang, W.; Zhang, Z.; Li, Y.; Si, F. Photocatalytic degradation of MB dye by the magnetically separable 3D flower- like Fe_3O_4/SiO_2/MnO_2/BiOBr-Bi photocatalyst. *J. Alloys Compd.* **2021**, *861*, 158256. [CrossRef]

152. Pozzo, R.L.; Baltanás, M.A.; Cassano, A.E. Supported titanium oxide as photocatalyst in water decontamination: State of the art. *Catal. Today* **1997**, *39*, 219–231. [CrossRef]

153. Zhu, Z.; Lu, Z.; Wang, D.; Tang, X.; Yan, Y.; Shi, W.; Wang, Y.; Gao, N.; Yao, X.; Dong, H. Construction of high-dispersed Ag/Fe_3O_4/g-C_3N_4 photocatalyst by selective photo-deposition and improved photocatalytic activity. *Appl. Catal. B Environ.* **2016**, *182*, 115–122. [CrossRef]

154. Zhao, X.; Wang, R.; Lu, Z.; Wang, W.; Yan, Y. Dual sensitization effect and conductive structure of Fe_3O_4@$mTiO_2$/C photocatalyst towards superior photodegradation activity for bisphenol A under visible light. *J. Photochem. Photobiol. A Chem.* **2019**, *382*, 111902. [CrossRef]

155. Tan, J.; Wang, X.; Hou, W.; Zhang, X.; Liu, L.; Ye, J.; Wang, D. Fabrication of Fe_3O_4@graphene/TiO_2 nanohybrid with enhanced photocatalytic activity for isopropanol degradation. *J. Alloys Compd.* **2019**, *792*, 918–927. [CrossRef]

156. Ji, H.Y.; Jing, X.C.; Xu, Y.G.; Yan, J.; Li, H.P.; Li, Y.P.; Huang, L.Y.; Zhang, Q.; Xu, H.; Li, H.M. Magnetic g-C_3N_4/$NiFe_2O_4$ hybrids with enhanced photocatalytic activity. *RSC Adv.* **2015**, *5*, 57960–57967. [CrossRef]

157. Shen, J.; Zhou, Y.; Huang, J.; Zhu, Y.; Zhu, J.; Yang, X.; Chen, W.; Yao, Y.; Qian, S.; Jiang, H.; et al. In-situ SERS monitoring of reaction catalyzed by multifunctional Fe_3O_4@TiO_2@Ag-Au microspheres. *Appl. Catal. B Environ.* **2017**, *205*, 11–18. [CrossRef]

158. Singh, P.; Sudhaik, A.; Raizada, P.; Shandilya, P.; Sharma, R.; Hosseini-Bandegharaei, A. Photocatalytic performance and quick recovery of BiOI/Fe_3O_4@graphene oxide ternary photocatalyst for photodegradation of 2,4-dintirophenol under visible light. *Mater. Today Chem.* **2019**, *12*, 85–95. [CrossRef]

159. Paul, A.; Dhar, S.S. Designing $Cu_2V_2O_7$/$CoFe_2O_4$/g-C_3N_4 ternary nanocomposite: A high performance magnetically recyclable photocatalyst in the reduction of 4-nitrophenol to 4-aminophenol. *J. Solid State Chem.* **2020**, *290*, 121563. [CrossRef]

160. Li, Y.; Li, L.; Hu, J.; Yan, L. A spray pyrolysis synthesis of $MnFe_2O_4$/SnO_2 yolk/shell composites for magnetically recyclable photocatalyst. *Mater. Lett.* **2017**, *199*, 135–138. [CrossRef]

161. Tariq, N.; Fatima, R.; Zulfiqar, S.; Rahman, A.; Warsi, M.F.; Shakir, I. Synthesis and characterization of MoO_3/$CoFe_2O_4$ nanocomposite for photocatalytic applications. *Ceram. Int.* **2020**, *46*, 21596–21603. [CrossRef]

162. Ma, M.; Chen, Y.; Tong, Z.; Liu, Y.; Ma, Y.; Wang, R.; Bi, Y.; Liao, Z. Research progress of magnetic bismuth-based materials in photocatalysis: A review. *J. Alloys Compd.* **2021**, *886*, 161096. [CrossRef]

163. Vaiano, V.; Sacco, O.; Sannino, D.; Stoller, M.; Ciambelli, P.; Chianese, A. Photo-catalytic Removal of Phenol by Ferromagnetic N-TiO_2/SiO_2/Fe_3O_4 Nanoparticles in presence of Visible Light Irradiation. *Chem. Eng. Trans.* **2016**, *47*, 235–240.

164. Hesas, R.H.; Baei, M.S.; Rostami, H.; Gardy, J.; Hassanpour, A. An investigation on the capability of magnetically separable Fe_3O_4/mordenite zeolite for refinery oily wastewater purification. *J. Environ. Manag.* **2019**, *241*, 525–534. [CrossRef]

165. Zhang, J.; Ma, Z. Flower-like Ag_2MoO_4/Bi_2MoO_6 heterojunctions with enhanced photocatalytic activity under visible light irradiation. *J. Taiwan Inst. Chem. Eng.* **2017**, *71*, 156–164. [CrossRef]

166. Liu, X.; Gu, S.; Zhao, Y.; Zhou, G.; Li, W. $BiVO_4$, Bi_2WO_6 and Bi_2MoO_6 photocatalysis: A brief review. *J. Mater. Sci. Technol.* **2020**, *56*, 45–68. [CrossRef]

167. Betancourt-Cantera, L.G.; Fuentes, K.M.; Bolarín-Miró, A.M.; Aldabe-Bilmes, S.; Cortés-Escobedo, C.A.; Sánchez-De Jesús, F. Enhanced photocatalytic activity of $BiFeO_3$ for water remediation via the addition of Ni^{2+}. *Mater. Res. Bull.* **2020**, *132*, 111012. [CrossRef]

168. Tao, R.; Li, X.; Li, X.; Liu, S.; Shao, C.; Liu, Y. Discrete heterojunction nanofibers of $BiFeO_3$/Bi_2WO_6: Novel architecture for effective charge separation and enhanced photocatalytic performance. *J. Colloid Interface Sci.* **2020**, *572*, 257–268. [CrossRef]

169. Cirkovic, J.; Radojkovic, A.; Golic, D.L.; Tasic, N.; Cizmic, M.; Brankovic, G.; Brankovic, Z. Visible-light photocatalytic degradation of mordant blue 9 by single-phase $BiFeO_3$ nanoparticles. *J. Environ. Chem. Eng.* **2021**, *9*, 104587. [CrossRef]

170. Haruna, A.; Abdulkadir, I.; Idris, S.O. Photocatalytic activity and doping effects of $BiFeO_3$ nanoparticles in model organic dyes. *Heliyon* **2020**, *6*, 03237. [CrossRef] [PubMed]

171. Cadenbach, T.; Benitez, M.J.; Morales, A.L.; Costa Vera, C.; Lascano, L.; Quiroz, F.; Debut, A.; Vizuete, K. Nanocasting synthesis of $BiFeO_3$ nanoparticles with enhanced visible-light photocatalytic activity. *Beilstein J. Nanotechnol.* **2020**, *11*, 1822–1833. [CrossRef] [PubMed]

172. Zhu, C.; Chen, Z.; Zhong, C.; Lu, Z. Facile synthesis of $BiFeO_3$ nanosheets with enhanced visible-light photocatalytic activity. *J. Mater. Sci. Mater. Electron.* **2017**, *29*, 4817–4829. [CrossRef]

173. Li, Y.A.; Zhang, X.; Chen, L.; Sun, H.; Zhang, H.; Si, W.; Wang, W.; Wang, L.; Li, J. Enhanced magnetic and photocatalytic properties of BiFeO$_3$ nanotubes with ultrathin wall thickness. *Vacuum* **2021**, *184*, 109867. [CrossRef]

174. Dmitriev, A.V.; Vladimirova, E.V.; Kandaurov, M.V.; Kellerman, D.G.; Kuznetsov, M.V.; Buldakova, L.U.; Samigullina, R.F. Synthesis of hollow spheres of BiFeO$_3$ from nitrate solutions with tartaric acid: Morphology and magnetic properties. *J. Alloys Compd.* **2019**, *777*, 586–592. [CrossRef]

175. Li, X.; Tang, Z.; Ma, H.; Wu, F.; Jian, R. PVP-assisted hydrothermal synthesis and photocatalytic activity of single-crystalline BiFeO$_3$ nanorods. *Appl. Phys. A* **2019**, *125*, 598. [CrossRef]

176. Bharathkumar, S.; Sakar, M.; Vinod, R.; Balakumar, S. Versatility of electrospinning in the fabrication of fibrous mat and mesh nanostructures of bismuth ferrite (BiFeO$_3$) and their magnetic and photocatalytic activities. *Phys. Chem. Chem. Phys.* **2015**, *17*, 17745–17754. [CrossRef]

177. Guo, F.; Wang, L.; Sun, H.; Li, M.; Shi, W. High-efficiency photocatalytic water splitting by a N-doped porous g-C$_3$N$_4$ nanosheet polymer photocatalyst derived from urea and N, N-dimethylformamide. *Inorg. Chem. Front.* **2020**, *7*, 1770–1779. [CrossRef]

178. Li, X.; Li, F.; Lu, X.; Zuo, S.; Li, Z.; Yao, C.; Ni, C. Microwave hydrothermal synthesis of BiP$_{1-x}$V$_x$O$_4$/attapulgite nanocomposite with efficient photocatalytic performance for deep desulfurization. *Powder Technol.* **2018**, *327*, 467–475. [CrossRef]

179. Shi, W.; Li, M.; Huang, X.; Ren, H.; Guo, F.; Tang, Y.; Lu, C. Construction of CuBi$_2$O$_4$/ Bi$_2$MoO$_6$ p-n heterojunction with nanosheets-on-microrods structure for improved photocatalytic activity towards broad spectrum antibiotics degradation. *Chem. Eng. J.* **2020**, *394*, 125009. [CrossRef]

180. Dieu Cam, N.T.; Pham, H.D.; Pham, T.D.; Thu Phuong, T.T.; Van Hoang, C.; Thanh Tung, M.H.; Trung, N.T.; Huong, N.T.; Thu Hien, T.T. Novel photocatalytic performance of magnetically recoverable MnFe$_2$O$_4$/BiVO$_4$ for polluted antibiotics degradation. *Ceram. Int.* **2001**, *47*, 1686–1692. [CrossRef]

181. Sakhare, P.A.; Pawar, S.S.; Bhat, T.S.; Yadav, S.D.; Patil, G.R.; Patil, P.S.; Sheikh, A.D. Magnetically recoverable BiVO$_4$/NiFe$_2$O$_4$ nanocomposite photocatalyst for efficient detoxification of polluted water under collected sunlight. *Mater. Res. Bull.* **2020**, *129*, 110908. [CrossRef]

182. Rohani Bastami, T.; Ahmadpour, A.; Ahmadi Hekmatikar, F. Synthesis of Fe$_3$O$_4$/Bi$_2$WO$_6$ nanohybrid for the photocatalytic degradation of pharmaceutical ibuprofen under solar light. *J. Ind. Eng. Chem.* **2017**, *51*, 244–254. [CrossRef]

183. Xiu, Z.; Cao, Y.; Xing, Z.; Zhao, T.; Li, Z.; Zhou, W. Wide spectral response photothermal catalysis-fenton coupling systems with 3D hierarchical Fe$_3$O$_4$/Ag/Bi$_2$MoO$_6$ ternary hetero-superstructural magnetic microspheres for efficient high-toxic organic pollutants removal. *J. Colloid Interface Sci.* **2019**, *533*, 24–33. [CrossRef] [PubMed]

184. Ren, X.; Gao, M.; Zhang, Y.; Zhang, Z.; Cao, X.; Wang, B.; Wang, X. Photocatalytic reduction of CO$_2$ on BiOX: Effect of halogen element type and surface oxygen vacancy mediated mechanism. *Appl. Catal. B Environ.* **2020**, *274*, 119063. [CrossRef]

185. Wang, Z.; Chu, Z.; Dong, C.; Wang, Z.; Yao, S.; Gao, H.; Liu, Z.; Liu, Y.; Yang, B.; Zhang, H. Ultrathin BiOX (X = Cl, Br, I) nanosheets with exposed {001} facets for photocatalysis. *ACS Appl. Nano Mater.* **2020**, *3*, 1981–1991. [CrossRef]

186. Li, Z.; Huang, G.; Liu, K.; Tang, X.; Peng, Q.; Huang, J.; Ao, M.; Zhang, G. Hierarchical BiOX (X = Cl, Br, I) microrods derived from bismuth-MOFs: In situ synthesis, photocatalytic activity and mechanism. *J. Clean. Prod.* **2020**, *272*, 122892. [CrossRef]

187. Wang, L.; Liu, G.P.; Wang, B.; Chen, X.; Wang, C.T.; Lin, Z.X.; Xia, J.X.; Li, H.M. Oxygen vacancies engineering-mediated BiOBr atomic layers for boosting visible light-driven photocatalytic CO$_2$ reduction. *Sol. RRL* **2020**, *5*, 2000480. [CrossRef]

188. Cao, L.; Ma, D.; Zhou, Z.; Xu, C.; Cao, C.; Zhao, P.; Huang, Q. Efficient photocatalytic degradation of herbicide glyphosate in water by magnetically separable and recyclable BiOBr/Fe$_3$O$_4$ nanocomposites under visible light irradiation. *Chem. Eng. J.* **2019**, *368*, 212–222. [CrossRef]

189. Li, X.; Wang, L.; Zhang, L.; Zhuo, S. A facile route to the synthesis of magnetically separable BiOBr/NiFe$_2$O$_4$ composites with enhanced photocatalytic performance. *Appl. Surf. Sci.* **2017**, *419*, 586–594. [CrossRef]

190. Li, X.; Xu, H.; Wang, L.; Zhang, L.; Cao, X.; Guo, Y. Spinel NiFe$_2$O$_4$ nanoparticles decorated BiOBr nanosheets for improving the photocatalytic degradation of organic dye pollutants. *J. Taiwan Inst. Chem. Eng.* **2018**, *85*, 257–264. [CrossRef]

191. Sin, J.C.; Lam, S.M.; Zeng, H.; Lin, H.; Li, H.; Tham, K.O.; Mohamed, A.R.; Lim, J.W.; Qin, Z. Magnetic NiFe$_2$O$_4$ nanoparticles decorated on N-doped BiOBr nanosheets for expeditious visible light photocatalytic phenol degradation and hexavalent chromium reduction via a Z-scheme heterojunction mechanism. *Appl. Surf. Sci.* **2021**, *559*, 149966. [CrossRef]

192. Ma, W.; Chen, L.; Zhu, Y.; Dai, J.; Yan, Y.; Li, C. Facile synthesis of the magnetic BiOCl/ ZnFe$_2$O$_4$ heterostructures with enhanced photocatalytic activity under visible- light irradiation. *Colloids Surf. A* **2016**, *508*, 135–141. [CrossRef]

193. Zhou, P.; Zhang, A.; Zhang, D.; Feng, C.; Su, S.; Zhang, X.; Xiang, J.; Chen, G.; Wang, Y. Efficient removal of Hg0 from simulated flue gas by novel magnetic Ag$_2$WO$_4$/BiOI/CoFe$_2$O$_4$ photocatalysts. *Chem. Eng. J.* **2019**, *373*, 780–791. [CrossRef]

194. Zhang, A.; Zhou, P.; Zhang, X.; Li, H.; Wang, Y.; Sun, Z.; Xiang, J.; Su, S.; Liu, Z. Insights into efficient removal of gaseous Hg0 using AgIO$_3$-Modified BiOI/CoFe$_2$O$_4$ composites through photocatalytic oxidation. *Energ. Fuel* **2019**, *33*, 12538–12548. [CrossRef]

195. Shan, B.; Zhao, Y.; Li, Y.; Wang, H.; Chen, R.; Li, M. High-quality dual-plasmonic Au@Cu$_{2-x}$Se nanocrescents with precise Cu$_{2-x}$Se domain size control and tunable optical properties in the second near-infrared biowindow. *Chem. Mater.* **2019**, *31*, 9875–9886. [CrossRef]

196. Shao, B.; Liu, X.; Liu, Z.; Zeng, G.; Liang, Q.; Liang, C.; Cheng, Y.; Zhang, W.; Liu, Y.; Gong, S. A novel double Z-scheme photocatalyst Ag$_3$PO$_4$/Bi$_2$S$_3$/Bi$_2$O$_3$ with enhanced visible-light photocatalytic performance for antibiotic degradation. *Chem. Eng. J.* **2019**, *368*, 730–745. [CrossRef]

197. Li, S.; Wang, Z.; Zhang, X.; Zhao, J.; Hu, Z.; Wang, Z.; Xie, X. Preparation of magnetic nanosphere/nanorod/nanosheet-like Fe_3O_4/Bi_2S_3/BiOBr with enhanced (001) and (110) facets to photodegrade diclofenac and ibuprofen under visible LED light irradiation. *Chem. Eng. J.* **2019**, *378*, 122169. [CrossRef]

198. Cong, Y.Q.; Ji, Y.; Ge, Y.H.; Jin, H.; Zhang, Y.; Wang, Q. Fabrication of 3D Bi_2O_3-BiOI heterojunction by a simple dipping method: Highly enhanced visible-light photoelectrocatalytic activity. *Chem. Eng. J.* **2017**, *307*, 572–582. [CrossRef]

199. Abbasi, Z.; Farrokhnia, A.; Garcia-Lopez, E.I.; Shoushtari, M.Z. Superparamagnetic recoverable flowerlike Fe_3O_4@Bi_2O_3 core-shell with g-C_3N_4 sheet nanocomposite: Synthesis, characterization, mechanism and kinetic study of photo-catalytic activity. *J. Mater. Sci. Mater. Electron.* **2019**, *31*, 1022–1033. [CrossRef]

200. Gao, N.; Lu, Z.; Zhao, X.; Zhu, Z.; Wang, Y.; Wang, D.; Hua, Z.; Li, C.; Huo, P.; Song, M. Enhanced photocatalytic activity of a double conductive C/Fe_3O_4/Bi_2O_3 composite photocatalyst based on biomass. *Chem. Eng. J.* **2016**, *304*, 351–361. [CrossRef]

201. Falletta, E.; Longhi, M.; Di Michele, A.; Boffito, D.C.; Bianchi, C.L. Floatable graphitic carbon nitride/alginate beads for the photodegradation of organic pollutants under solar light irradiation. *J. Clean. Prod.* **2022**, 133641. [CrossRef]

202. Wang, X.; Wang, X.; Zhao, J.; Song, J.; Zhou, L.; Wang, J.; Tong, X.; Chen, Y. An alternative to in situ photocatalytic degradation of microcystin-LR by worm-like N, P co-doped TiO_2/expanded graphite by carbon layer (NPT-EGC) floating composites. *Appl. Catal. B Environ.* **2017**, *206*, 479–489. [CrossRef]

203. Zhou, W.; Li, W.; Wang, J.Q.; Qu, Y.; Yang, Y.; Xie, Y.; Zhang, K.; Wang, L.; Fu, H.; Zhao, D. Ordered Mesoporous Black TiO_2 as Highly Efficient Hydrogen Evolution Photo-catalyst. *J. Am. Chem. Soc.* **2014**, *136*, 9280–9283. [CrossRef] [PubMed]

204. Djellabi, R.; Zhao, X.; Frias Ordonez, M.; Falletta, E.; Bianchi, C.L. Comparison of the photoactivity of several semiconductor oxides in floating aerogel and suspension systems towards the reduction of Cr(VI) under visible light. *Chemosphere* **2001**, *281*, 130839. [CrossRef] [PubMed]

205. Wang, S.; Zhang, Y.; Zhang, T.; Dong, F.; Huang, H. Readily attainable spongy foam photocatalyst for promising practical photocatalysis. *Appl. Catal. B Environ.* **2017**, *208*, 75–81. [CrossRef]

206. Chawla, H.; Saha, M.; Upadhyay, S.; Rohilla, J.; Ingole, P.P.; Sapi, A.; Szenti, I.; Yadav, M.; Lebedev, V.T.; Chandra, A.; et al. Enhanced photocatalytic activity and easy recovery of visible light active $MoSe_2$/$BiVO_4$ heterojunction immobilized on Luffa cylindrica—Experimental and DFT study. *Environ. Sci. Nano* **2021**, *8*, 3028. [CrossRef]

207. Huang, X.-H.; Hu, T.; Bu, H.; Li, W.X.; Li, Z.L.; Hu, H.J.; Chen, W.Z.; Lin, Y.; Jiang, G.B. Transparent floatable magnetic alginate sphere used as photocatalysts carrier for im-proving photocatalytic efficiency and recycling convenience. *Carbohydr. Polym.* **2021**, *254*, 117281. [CrossRef]

208. Said, K.A.M.; Ismail, A.F.; Karim, Z.A.; Abdullah, M.S.; Hafeez, A. A review of tech-nologies for the phenolic compounds recovery and phenol removal from wastewater. *Process Saf. Environ. Prot.* **2021**, *151*, 257–289. [CrossRef]

209. Rawindran, H.; Lim, J.W.; Goh, P.S.; Subramaniam, M.N.; Ismail, A.F.; Arzhandi, M.R.D. Simultaneous separation and degradation of surfactants laden in produced water using PVDF/TiO_2 photocatalytic membrane. *J. Clean. Prod.* **2019**, *221*, 490–501. [CrossRef]

210. Algamdi, M.S.; Alsohaimi, I.H.; Lawler, J.; Ali, H.M.; Aldawsari, A.M.; Hassan, H.M.A. Fabrication of graphene oxide incorporated polyethersulfone hybrid ultra-filtration membranes for humic acid removal. *Sep. Purif. Technol.* **2019**, *223*, 17–23. [CrossRef]

211. Zhou, K.-G.; McManus, D.; Prestat, E.; Zhong, X.; Shin, Y.; Zhang, H.-L.; Haigh, S.; Casiraghi, C. Self-catalytic membrane photo-reactor made of carbon nitride nanosheets. *J. Mater. Chem. A Mater. Energy Sustain.* **2016**, *4*, 11666–11671. [CrossRef]

212. Dzinun, H.; Othman, M.H.D.; Ismail, A.F.; Puteh, M.H.; Rahman, M.A.; Jaafar, J. Photocatalytic degradation of nonylphenol using coextruded dual-layer hollowfibre membranes incorporated with a different ratio of TiO2/PVDF. *React. Funct. Polym.* **2016**, *99*, 80–87. [CrossRef]

213. Dzinun, H.; Othman, M.H.D.; Ismail, A.F.; Puteh, M.H.; Rahman, M.A.; Jaafar, J.; Adrus, N.; Hashim, N.A. Antifouling behavior and separation performance of immobilized TiO_2 in dual layer hollow fiber membranes. *Polym. Eng. Sci.* **2017**, *58*, 1636–1643. [CrossRef]

214. Dzinun, H.; Othman, M.H.D.; Ismail, A.F. Photocatalytic performance ofTiO_2/Clinoptilolite: Comparison study in suspension and hybrid photocatalytic membrane reactor. *Chemosphere* **2019**, *228*, 241–248. [CrossRef] [PubMed]

215. Sharma, N.K.; Philip, L. Combined biological and photocatalytic treatment of real coke oven wastewater. *Chem. Eng. J.* **2016**, *295*, 20–28. [CrossRef]

216. Salim, N.E.; Jaafar, J.; Ismail, A.F.; Othman, M.H.D.; Rahman, M.A.; Yusof, N.; Qtaishat, M.; Matsuura, T.; Aziz, F.; Salleh, W.N.W. Preparation and characterization of hydrophilic surface modifier macro-molecule modified poly (ether sulfone) photocatalytic membrane for phenol removal. *Chem. Eng. J.* **2018**, *335*, 236–247. [CrossRef]

217. Salim, N.E.; Nor, N.A.M.; Jaafar, J.; Ismail, A.F.; Qtaishat, M.R.; Matsuura, T.; Othman, M.H.D.; Rahman, M.A.; Aziz, F.; Yusof, N. Effects of hydrophilic surface macromolecule modifier loading on PES/O-g-C_3N_4 hybrid photocatalytic membrane for phenol removal. *Appl. Surf. Sci.* **2019**, *465*, 180–191. [CrossRef]